

Logarithmically slow domain growth in nonrandomly frustrated systems: Ising models with competing interactions

Joel D. Shore,* Mark Holzer, and James P. Sethna

Laboratory of Atomic and Solid State Physics, Cornell University, Ithaca, New York 14853-2501

(Received 15 April 1992)

We study the growth (“coarsening”) of domains following a quench from infinite temperature to a temperature T below the ordering transition. The model we consider is an Ising ferromagnet on a square or cubic lattice with weak next-nearest-neighbor antiferromagnetic (AFM) bonds and single-spin-flip dynamics. The AFM bonds introduce free-energy barriers to coarsening and thus greatly slow the dynamics. In two dimensions, the barriers are independent of the characteristic length scale $L(t)$, and therefore the long-time ($t \rightarrow \infty$) growth of $L(t)$ still obeys the standard $t^{1/2}$ law. However, in three dimensions, a simple physical argument suggests that for quenches below the corner-rounding transition temperature, T_{CR} , the barriers are proportional to $L(t)$ and thus grow as the system coarsens. Quenches to $T < T_{CR}$ should, therefore, lead to $L(t) \sim \ln(t)$ at long times. Our argument for logarithmic growth rests on the assertion that the mechanism by which the system coarsens involves the creation of a step across a flat interface, which below T_{CR} costs a free energy proportional to its length. We test this assertion numerically in two ways: First, we perform Monte Carlo simulations of the shrinking of a cubic domain of up spins in a larger sea of down spins. These simulations show that, below T_{CR} , the time to shrink the domain grows exponentially with the domain size L . This confirms that the free-energy barrier, $F_B(L, T)$, to shrinking the domain is indeed proportional to L . We find excellent agreement between our numerical data and an approximate analytic expression for $F_B(L, T)$. Second, to be sure that the coarsening system cannot somehow find paths around these barriers, we perform Monte Carlo simulations of the coarsening process itself and find strong support for $L(t) \sim \ln(t)$ at long times. Above T_{CR} the step free energy vanishes and coarsening proceeds via the standard $t^{1/2}$ law. Thus, the corner-rounding transition marks the boundary between different growth laws for coarsening in much the same way that the roughening transition separates different regimes of crystal growth. We also find logarithmic coarsening following a quench in a two-dimensional “tiling” system, which models the corner-rounding transition of a [111] interface in our three-dimensional model. However, if instead of quenching, we cool the system slowly at a constant rate Γ , we find the final length scale L to have a power-law dependence on $1/\Gamma$, i.e., $L \sim \Gamma^{-1/4}$, in accordance with a theoretical argument. The predictions concerning the dynamics of the tiling model should, in principle, be experimentally testable for a [111] interface of sodium chloride.

I. INTRODUCTION

It is known that in systems with externally imposed disorder (i.e., randomness in their Hamiltonians), the dynamics of ordering can be greatly slowed because of free-energy barriers which grow with the size of the correlated regions.^{1,2,3} Motivated by the slow dynamics present in glasses (discussed in Appendix A), we have searched for model systems in which such diverging barriers, and the resulting slow dynamics, occur even *without* imposed disorder. We have found^{4,5} two such closely related models which we present in this paper. In these models, the length scale with which the barriers diverge is not, however, the equilibrium correlation length, but rather the characteristic length scale $L(t)$ of the domains in a coarsening system. By a coarsening system we mean one which has been quenched from above to below its ordering transition and is thus far out of equilibrium. We will argue that the barriers to coarsening grow linearly with $L(t)$, and that, as a result, $L(t)$ grows only logarithmically with time t following a deep quench. Before introducing the first model that we study, let us review the relevant work on coarsening.

A. Coarsening: A brief review (Ref. 6)

When an Ising model is quenched from a temperature well above its critical temperature, T_c , to a temperature below T_c , the system finds itself in a disordered configuration at a temperature which favors ordering. At first, local regions of a few spins order. However, since the ground state is up-down degenerate, some local regions will order up and some down. Thus, after a short time, one has a patchwork of up and down domains. Since there is an interfacial free-energy cost associated with the total length (or, in three dimensions, the total surface area) of the boundary between domains, this patchwork will evolve over time so as to decrease the total boundary. This process by which the system orders over larger and larger length scales is called “coarsening,” although it is also commonly referred to as “domain growth.”

Coarsening is ubiquitous in nature. Examples include the coarsening of foams (e.g., bubbles in the “head” of beer), the coarsening of the grains in a metal during the annealing process, the ordering of a binary alloy following a quench from above to below its order-disorder tran-

sition, and the phase separation of a binary fluid or alloy following a quench from the one-phase to the two-phase region of its phase diagram.

In many ways, a coarsening system at late times is analogous to an equilibrium system near a critical point. For example, the coarsening system can be characterized by a single "characteristic length scale" $L(t)$ which generally grows with some power of the time

$$L(t) \sim t^n. \quad (1.1)$$

Since at late times this length scale will be macroscopic, one might expect that, just as in static critical phenomena, the exponent n of the scaling will be independent of certain microscopic details of the system (i.e., of the lattice, the Hamiltonian, and the dynamics), and that there will thus be only a few universality classes. Two such universality classes have been delineated. The first, with $n = \frac{1}{2}$, is called Lifshitz-Allen-Cahn,^{7,8} or "curvature-driven," growth and occurs in many systems in which the order parameter is not conserved by the dynamics. Physical examples of this class include ordering in binary alloys, grain growth in metals, and coarsening of foams. The second, slower class, with $n = \frac{1}{3}$, is called Lifshitz-Slyozov⁹ growth, and occurs when the order parameter is conserved by the dynamics. The primary example of this class is spinodal decomposition, the process of phase separation in a binary fluid or alloy quenched from its one-phase region (where the atoms mix) into the two-phase region (where they separate). That the order parameter in such a system must be conserved follows from the fact that the total number of atoms or molecules of each type is not changing with time.

Are these the only universality classes for coarsening? An important lesson from static critical phenomena is that universality is a subtle business. That is, not all details of the system are irrelevant, and distinguishing the relevant from the irrelevant perturbations is not always obvious. While it is very appealing to imagine that all models fall into one of these two universality classes, there is no *a priori* reason why we should expect this to be the case. In fact, as we will discuss further below, it is already known that systems with imposed disorder, such as the random-field Ising model or an Ising model with dilute impurities, will have logarithmically slow coarsening (" $n = 0$ ").

During the past decade, there have been various claims that, even in certain models without randomness, coarsening would not obey the $t^{1/2}$ or $t^{1/3}$ laws, but instead obey $L(t) \sim \ln(t)$. In particular, there were claims that in a d -dimensional system with $Q \geq d + 1$ degenerate phases (e.g., a Q -state Potts model),^{7,10} and in an Ising model with spin-exchange dynamics,¹¹ the growth of $L(t)$ would be logarithmic, at least at low temperatures. For a while, these claims could not be disproved since the numerical evidence was ambiguous due to long-time transients and finite-size effects. In particular, the fact that domains in these coarsening models were found to freeze entirely at zero temperature,¹² and to grow only slowly at very low temperatures, was taken by some as support for these claims. However, large Monte Carlo simulations, bolstered by more careful theoretical arguments, eventually

showed that the long-time growth in these models obeys the naively expected power laws,¹³⁻¹⁷ at least in two dimensions.

Two points should be drawn from this historical perspective. First, one must be careful when determining the growth law numerically. The primary reason that these controversies occurred in the first place is that numerical simulations often give ambiguous results because they are hampered by both finite-size effects and initial transients. The former can become a problem even when L is only a fraction of the system's linear dimension.¹⁴ The latter can affect results even out to quite late times, particularly when there are energy barriers present which cause freezing after a quench to $T = 0$.

Second, the relation between such zero-temperature freezing and logarithmic growth has been widely misunderstood. Originally, there was the belief that zero-temperature freezing would imply logarithmic coarsening at low T . In light of the evidence showing this is not necessarily the case, the pendulum of opinion seems to have swung the other way, with the assumption made (at least implicitly) that zero-temperature freezing is always an uninteresting phenomenon.¹⁸ In fact, there seems to be growing conviction that the standard $t^{1/2}$ and $t^{1/3}$ laws will hold universally (at $T \neq 0$), independent of almost any details of the Hamiltonian save randomness. This conviction has been stated, with varying degrees of generality, by several authors.¹⁹ It is important to note, however, that no one has demonstrated the degree to which universality should apply. The belief that it should apply so broadly is based mainly upon the growing number of systems in which these laws hold and the lack of any counterexamples.

It is Lai, Mazenko, and Valls³ who have stated clearly when to expect logarithmic growth. They distinguish four different classes of systems on the basis of how the free-energy barriers to coarsening grow with $L(t)$.²⁰ Emphasizing what we think is most fundamental, namely, the differential form for the growth of $L(t)$, we present here (in a suitably modified form) the delineation of these classes. For definiteness, let us consider the differential equation for the case of curvature-driven growth:

$$\frac{dL}{dt} = \frac{a(L, T)}{L}. \quad (1.2)$$

(Completely analogous arguments follow for the Lifshitz-Slyozov case by replacing the L in the denominator by L^2 .) The four classes can then be distinguished by the behavior of $a(L, T)$.

Class 1, in which $a(L, T)$ remains nonzero as $T \rightarrow 0$, consists of those systems which do not have energy barriers to coarsening and thus coarsen even at $T = 0$. The canonical example is the Ising model with spin-flip dynamics. (This class, Lai *et al.* point out, is actually unphysical since all known experimental examples of coarsening have elementary processes which involve activation over barriers.)

The other three classes all freeze at zero temperature (i.e., $a \rightarrow 0$ as $T \rightarrow 0$). Class 2 consists of systems whose energy barriers are independent of L . For example, if there is only one such barrier height, F_B , then we can

write $a(L, T) = a_0 e^{-F_B/T}$. (Throughout this paper, we use units such that $k_B = 1$.) Integrating Eq. (1.2) for this case gives

$$L(t) = \sqrt{L_0^2 + a_0 t / \tau(T)}, \quad (1.3)$$

where $\tau(T) = e^{F_B/T}$ is the characteristic time to surmount the barriers. In such systems, coarsening will be slow, with $L(t) \approx L_0$, for times t short compared to τ ; however, on time scales long compared to τ , activation over the barriers will be common and one finds normal power-law growth, $L(t) \sim t^{1/2}$ (albeit, with a strongly temperature-dependent prefactor).

Class 3 and 4 systems are those in which the barriers grow with L . Class 3 refers to the case where the barriers grow linearly with L , while class 4 refers to the case where they grow like L^m with $m \neq 1$. Lai *et al.* note that all known examples of these two classes are systems with disorder, i.e., randomness in their Hamiltonians. An example of a system believed to be class 3 is the random-field Ising model, while spin glasses and the Ising model with random quenched impurities are thought to be class-4 systems. For class 3, we can write $a(L, T) = a_0 e^{-f_B L/T}$, where f_B is a free-energy barrier per unit length. Integrating Eq. (1.2) then leads to a complicated expression, which at long times goes asymptotically to the form

$$L(t) \sim \frac{T}{f_B} \ln(t). \quad (1.4)$$

Likewise, for class 4, $L(t) \sim [\ln(t)]^{1/m}$ as $t \rightarrow \infty$.

B. Argument for logarithmic coarsening

In this paper, we will show, by example, that there exist models without randomness in their Hamiltonians which nonetheless have free-energy barriers that grow with the coarsening length (i.e., are in class 3 or 4), and thus have logarithmically slow dynamics.

1. Introduction to the model

To study the dynamics of a statistical mechanical model, we must specify two things: the Hamiltonian and the dynamical rule for evolving the system. The bulk of this paper (excluding Sec. IV) will consider a system whose Hamiltonian is simply the ferromagnetic Ising model on a square or cubic lattice in $d=2$ or 3 dimensions, with dynamical frustration²¹ added by introducing weak next-nearest-neighbor antiferromagnetic (AFM) bonds. The Hamiltonian is thus

$$H = -J_1 \sum_{\text{NN}} s_i s_j + J_2 \sum_{\text{NNN}} s_i s_j, \quad (1.5)$$

where the spins s_i take on the values $+1$ and -1 . The first sum is over all pairs of nearest neighbors (NN) while the second is over all pairs of next-nearest-neighbors (NNN). We have chosen our sign convention so that both J_1 and J_2 are positive when the NN bonds are ferromagnetic and the NNN bonds are antiferromagnetic. We will require that $J_1/J_2 > 2(d-1)$ so that the ground

state is ferromagnetic.²²

The dynamical evolution of the model will be governed by random-updating, single-spin-flip dynamics. This means that a spin is chosen at random and flipped with a probability P given by

$$P = \frac{e^{-\Delta E/T}}{1 + e^{-\Delta E/T}}, \quad (1.6)$$

where ΔE is the change in energy that flipping this spin would produce.²³ The updating rule we use, Eq. (1.6), is usually referred to as Glauber dynamics.²⁴ Metropolis dynamics²⁵ should give qualitatively similar results.

2. Expected behavior of the model in two and three dimensions

The following simple physical argument demonstrates that the NNN bonds introduce energy barriers to domain coarsening. Let us consider shrinking a droplet of, say, up spins immersed in a sea of down spins.

First, we consider a square droplet in a two-dimensional (2D) system as shown in Fig. 1(a). For simplicity, let us assume $T \ll J_1$ so that only spin flips which do not raise the J_1 energy are accepted. Without the NNN (J_2) bonds, such a square can shrink away without the system having to cross any energy barriers, since a corner flips for free, and then the edges can unravel for free. (This is why a nearest-neighbor Ising model will coarsen even at $T=0$.) However, the NNN bonds introduce an energy barrier of $4J_2$ to flipping a corner spin (shaded dark gray) since three of its four NNN spins (those spins diagonally away from it) are pointing down. Once the corner flips, the neighboring spins along the edge (shaded light gray) can flip for free (and the final spin to flip along the edge reduces the system's energy by $4J_1$). Therefore, shrinking the square involves surmount-

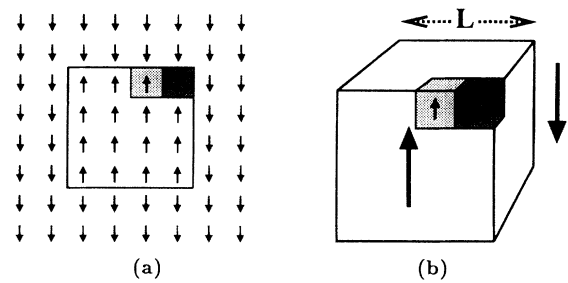


FIG. 1. (a) A square domain of “up” spins in a system of “down” spins, in two dimensions. The next-nearest-neighbor bonds introduce an energy barrier of $4J_2$ to flipping a corner spin (dark gray). As a result, it takes a time of order $e^{4J_2/T}$ to shrink the entire domain. (b) A cubic domain in three dimensions. (Here, for clarity, most of the individual spins have not been shown.) There is an energy barrier of $12J_2$ to flip a corner spin (dark gray) and a barrier of $4J_2$ to flip each spin along the edge (light gray). Thus, unlike in two dimensions, the total barrier to flip all the spins along an edge is proportional to the linear size, L , of the domain; and the time to shrink the domain is now exponential in L .

ing energy barriers of height $F_B = 4J_2$. Note that the barriers to be crossed are *independent* of the edge length L . For time scales smaller than a characteristic time $\tau = e^{4J_2/T}$, we expect little domain coarsening to occur. However, on time scales much longer than τ , such corner flips occur regularly and the $t^{1/2}$ law should be observed. (In the language of Lai, Mazenko, and Valls,³ this is a class-2 system.) Thus, although the dynamics is slowed, the behavior of the growth law at asymptotically long times is not changed. Because of this, the 2D case will be of little interest to us except insofar as it provides a nice contrast to the 3D case.²⁶

In three dimensions, the argument for the energy barriers to flipping a cube of linear size L , shown in Fig. 1(b), is made analogously. The energy barrier to flip a corner spin is now $12J_2$ because 9 of its 12 NNN spins are pointing down (as can be seen by counting the number of visible edges of the corner cube). However, the important feature which enters is that there is a barrier of $4J_2$ to flip each additional spin along the edge. Since to flip an entire edge requires that the corner spin flip and then each edge spin flip in turn, the barriers add and the total barrier to remove an entire edge is

$$F_B(L) = 4(L + 1)J_2. \quad (1.7)$$

(This is simply the energy difference between the initial state with the cubic domain and the state in which all but one of the spins along an edge of the cube have flipped. Once an entire edge has flipped, there are other smaller energy barriers which must be crossed to further shrink the cube. However, in the low- T or high- L limit, the largest of the barriers that must be crossed in sequence dominates the time to flip the cube.) We have already argued that barriers proportional to the length scale $L(t)$ will yield logarithmically slow coarsening at long times. A quick and dirty way to see this is to note that the time to flip a cube is $t = \tau_0 e^{4(L+1)J_2/T}$. Simply inverting this expression³ by solving for L tells us that the coarsening length grows as

$$L(t) \sim \frac{T}{4J_2} \ln(t/\tau_0). \quad (1.8)$$

3. Outline of the paper

Our argument for logarithmic growth in the 3D model has an appealing simplicity to it. Unfortunately, however, it is only suggestive and is far from a rigorous proof. In Secs. II and III, we will address the two major objections which we can envision.

(1) One can challenge our assertions concerning the barrier to shrinking a cubic domain. In particular, at nonzero temperatures, one must consider not energy barriers but, rather, *free-energy* barriers. The effects of entropy must be accounted for. In Sec. II, we will find, through both analytic work and simulations of shrinking cubes, that our argument indeed breaks down above a temperature T_{CR} , which we identify as the corner-rounding transition temperature previously studied in the context of equilibrium crystal shapes.²⁷ Only below this temperature does the free-energy barrier to depin a step

from an edge scale with the length of the edge. It is important to note that such a transition occurs only when one has the discreteness introduced by the lattice. Continuum models will not have the pinned phase (unless they explicitly contain a term to model this discreteness). This is why the possibility of logarithmically slow coarsening is overlooked by the Lifshitz-Allen-Cahn analysis.

(2) One can challenge the claim that the barriers we have identified to shrinking cubes imply logarithmic coarsening. The jump in logic from Eq. (1.7) to Eq. (1.8) is, indeed, a large gap in our argument: We have identified a special configuration in which there are energy barriers which scale with the length scale L ; however, we have not shown that, during the process of coarsening, the system will necessarily find itself in configurations in which it will have to cross these barriers in order to coarsen further. It is conceivable that the system could find a way around these barriers. To construct a proof that the barriers must be crossed is very difficult since it requires a detailed understanding of the spin configurations which form in a quench. Instead, in Sec. III, we will be content to give some brief arguments explaining why we think it is plausible that the barriers cannot be avoided, and then ultimately, as is most common in this field, we will perform numerical simulations of the quench to back up our arguments.

In Sec. IV, we introduce what we dub the “tiling model.” This is a 2D model for a [111] interface in our 3D Ising model. This model is itself describable as an Ising model on a triangular lattice, but has a more compelling visual representation as a tiling of the plane by rhombi of three different orientations. The same basic arguments for logarithmic coarsening should hold in this model. The model is a bit more obscure than, but has two clear advantages over, the 3D model. The first is that, since it is two dimensional, we can actually look at the configurations which the system is getting stuck in. The second is that since the larger J_1 energy scale is removed naturally by introducing a constraint on the allowed configurations, we can simulate the system out to times which correspond to energy barriers much larger than any elementary (single-spin-flip) energy barriers in the model. This makes it seem unlikely that the growth of $L(t)$ would resume power-law behavior at longer times.

In Sec. V, we summarize, and briefly discuss some open questions to be pursued.

Appendix A presents a brief discussion of the slow dynamics in glasses, our theoretical view on the matter,²⁸ and how this view motivated our search for logarithmically slow coarsening in systems without randomness. Appendix B gives a brief summary of how to most easily compute the energy of configurations in our 3D model. Appendix C contains a brief discussion on the implementation of the Monte Carlo algorithm. A discussion of the scaling and anisotropy of the correlation function for the coarsening simulations of Sec. III is presented in Appendix D.

Finally, we note that some of the work presented here has appeared elsewhere^{4,5} in abbreviated forms. A somewhat lengthier presentation than that given here can be found in Ref. 29.

II. ANALYSIS OF SHRINKING CUBES

A. Numerical simulations of shrinking squares and cubes

To investigate the free-energy barrier for shrinking square or cubic droplets at nonzero temperatures, we turn first to Monte Carlo simulations of this process. We start with the less interesting, 2D case. Figure 2 shows the results of Monte Carlo simulations for the time to shrink a square domain. (Details of the Monte Carlo algorithm are given in Appendix C.) Since this is an Arrhenius plot, activation over a constant free-energy barrier would give a straight line with the slope equal to the barrier height. Indeed, the low-temperature Monte Carlo data can be fit well to a straight line. The slope of the data is independent of the size of the domain, implying a free-energy barrier independent of domain size. Furthermore, the form

$$t = \tau_0(L) e^{4J_2/T} \quad (2.1)$$

with $\tau_0(L)$ as a free parameter gives fine fits to the data, thus demonstrating that the free-energy barrier is $4J_2$, as expected.

Figure 3 shows the time to flip the first edge of a cubic domain in three dimensions.³⁰ Again the low-temperature data are quite straight on this Arrhenius plot, thus indicating that shrinking a cube is also an activated process. However, in contrast to two dimensions,

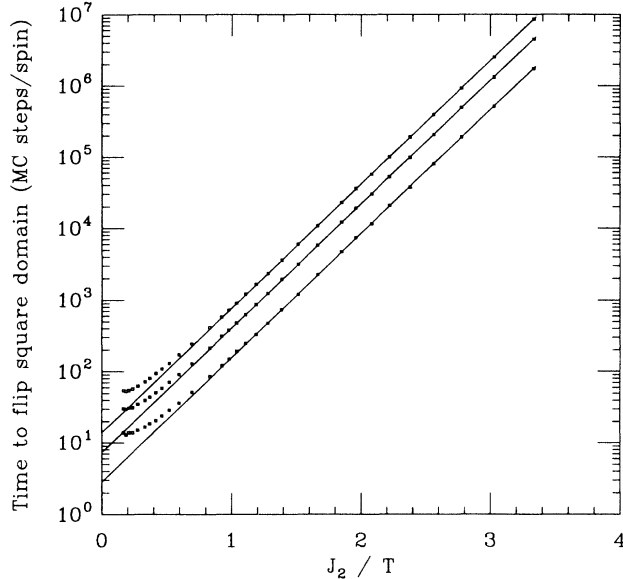


FIG. 2. Shrinking of a square domain in two dimensions. This shows the times to shrink a square domain vs J_2/T , as obtained from Monte Carlo simulations with $J_1/J_2=6$. The three sets of Monte Carlo data are for domains of size $L=4, 6$, and 8 (bottom to top). Each point is an average over 900 runs with standard error smaller than the symbol size. Lines are one-parameter fits to Eq. (2.1) using the ten lowest-temperature data points. (If we instead make the free-energy barrier F_B a free parameter too, we find $F_B/J_2=4.00\pm 0.01, 3.99\pm 0.01$, and 3.99 ± 0.01 for $L=4, 6$, and 8 , respectively.) This confirms that shrinking a square domain involves activation over barriers of height $4J_2$, independent of domain size.

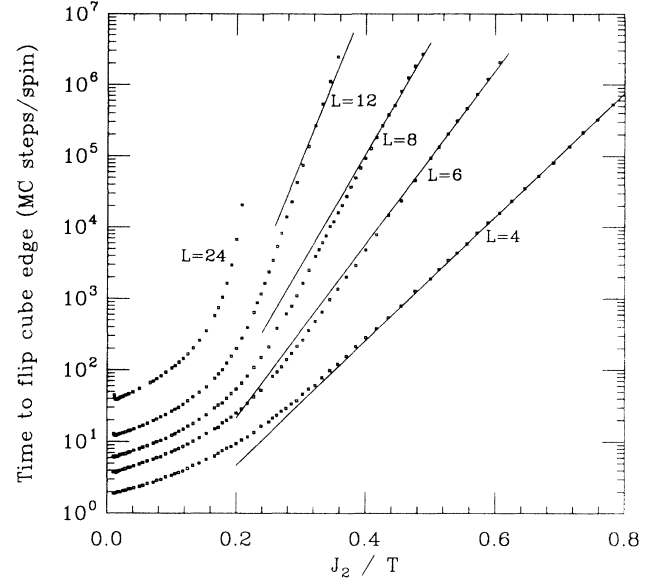


FIG. 3. Shrinking of a cubic domain in three dimensions. Shown is the time to flip the first edge of a cubic domain of size L vs J_2/T from Monte Carlo simulations for $J_1/J_2=100$. ($J_1/J_2=6$ yields results essentially indistinguishable from this for $T < 4J_2$. At higher temperatures the results for these two values of J_1/J_2 differ markedly.) Each point is an average over 900 or 1600 runs with standard error smaller than the symbol size. As expected, the slope of the data increases with cube size. For each value of L , except $L=24$, we show one-parameter fits to Eq. (2.2) using the 7–10 lowest-temperature points. For small L , the fits are quite good; but for $L=8$ and 12 , the fits are clearly inadequate.

here the slope, and thus the free-energy barrier, is clearly an increasing function of the size of the domain. In Fig. 3, we have tried a fit to the expected form

$$t = \tau_0(L) e^{4J_2(L+1)/T}, \quad (2.2)$$

with $\tau_0(L)$ as a free parameter. For $L=4$, the fit appears quite good at low temperatures, but for $L=6$ it is marginal, and for $L=8$ and especially $L=12$ the fit is clearly inadequate (down to the lowest temperatures we can reach).

The lack of agreement with the predicted zero-temperature barrier is not too surprising since we expect the free-energy barrier to decrease as the temperature is raised. (That this is the case will be shown in Sec. II B, and derives fundamentally from the fact discussed in Sec. II D that the barrier is a step free energy, which, being an equilibrium free energy, must decrease with temperature.) What may seem surprising at first is that the slope of the data is larger than the predicted slope of $4J_2(L+1)$, tempting us to conclude that the free-energy barrier is, in fact, *larger* than predicted. That this conclusion is incorrect can be seen by considering the general form for Arrhenius activation over a free-energy barrier $F_B(L, T)$:

$$t = \tau_0(L) e^{F_B(L, T)/T}. \quad (2.3)$$

Taking the logarithm of this expression and differentiating with respect to $1/T$, we get that the slope on an Arrhenius plot is

$$\frac{d[\ln(t)]}{d[1/T]} = F_B - T \frac{dF_B}{dT}. \quad (2.4)$$

If dF_B/dT is negative, the slope on the Arrhenius plot will be greater than the free-energy barrier. Physically this is because if the free-energy barrier increases as we lower the temperature, then the resulting rise in the activation time t is due partly to the direct consequence of the decrease in the temperature and partly to the fact that the barrier itself has increased. In fact, the right-hand side of Eq. (2.4) will be greater than the zero-temperature barrier, $F_B(L, T=0)$, if $F_B(L, T)$ is concave down over the region between 0 and T . We expect such negative concavity on general grounds since we anticipate that $dF_B/dT=0$ at $T=0$ and that it becomes negative for $T>0$. Thus, a steeper slope than $4J_2(L+1)$ is perfectly consistent with the notion that the free-energy barrier $F_B(L, T)$ is decreasing with temperature.

Returning to Fig. 3, we see that there are more features to explain at higher temperatures. For temperatures above $T \approx 6J_2$, the data appear to enter a regime where the free-energy barrier becomes roughly independent of size. In Sec. IID, we will explain that the temperature marking this change from an L -dependent barrier to an L -independent barrier occurs at the corner-rounding temperature, T_{CR} , of the associated equilibrium crystal shape problem.²⁷ This is then the temperature at which we expect our argument for logarithmic coarsening to break down. (The higher temperature of $T \approx 100J_2$, or more suggestively, $T \approx J_1$, at which the barrier appears to vanish altogether is most likely merely a quirk of our criterion for determining when the first edge of the cube has disappeared. This criterion becomes suspect once T/J_1 is large enough for there to be a significant probability of thermal fluctuations in equilibrium.) First, however, let us study in more detail the behavior of the time to flip an edge of a cubic domain in the low-temperature regime.

B. Analytic calculation of the time to flip an edge of a cube

The goal of this subsection is to derive an analytical expression to match the simulation results for flipping the first edge of a cube (Fig. 3). To get the total rate for flipping a cube edge, we must sum over the rates for all possible paths in configuration space which go from the state of a complete cube to one with spins along an entire edge (and perhaps other spins) flipped. The rate along any such path is just $\Gamma_i = \Gamma_{0i} e^{-E_i/T}$. Here, E_i is the energy barrier (the maximum energy above the initial configuration) along the given path and Γ_{0i} is a prefactor which we expect to have some weak temperature dependence. (In particular, Γ_{0i} should go to a nonzero constant in the limit $T \rightarrow 0$.)

At this point, it is useful to make an analogy with equilibrium statistical mechanics. The analogy is made by defining a barrier partition function Z_B as

$$Z_B \equiv \sum_i \exp(-E_i/T), \quad (2.5)$$

where the sum ranges over the barrier configurations (see Fig. 4), *not* all paths. The free-energy barrier F_B is then given by

$$F_B \equiv -T \ln(Z_B). \quad (2.6)$$

In terms of F_B , the average time to flip the spins along the edge of a cube can now be written as

$$t \equiv \frac{1}{\sum_i \Gamma_i} = \frac{1}{\bar{\Gamma}_0} \exp(F_B/T), \quad (2.7)$$

where

$$\bar{\Gamma}_0 \equiv \frac{\sum_i \Gamma_{0i} \exp(-E_i/T)}{Z_B}. \quad (2.8)$$

Unfortunately, computing the prefactor Γ_{0i} for each barrier configuration is prohibitive. Therefore, we will make the following approximation: We set $\bar{\Gamma}_0$ equal to an estimate of the prefactor Γ_{0i} for the *lowest* energy barrier. This estimate, in turn, is obtained by considering only flips of spins along an edge of the cube, occurring sequentially starting from one corner. The problem can then be formulated as a one-dimensional master equation, for which an exact solution can be obtained in the limit $L \rightarrow \infty$.²⁹ The expression for $\bar{\Gamma}_0$ thus found is

$$\bar{\Gamma}_0 = \frac{12(1 - e^{-4J_2/T})^2}{1 - e^{-4J_2/T} + e^{-12J_2/T}}. \quad (2.9)$$

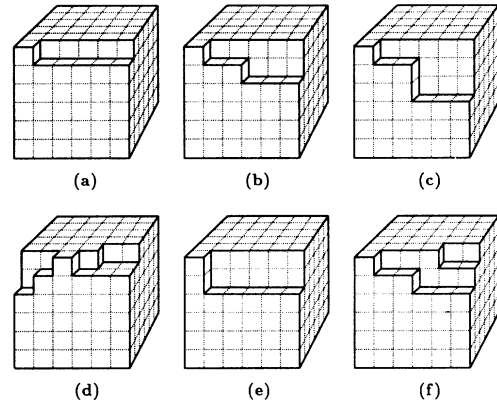


FIG. 4. Various configurations of a cube with all but one spin along the top edge flipped. (a) shows the configuration with the lowest possible energy barrier of $4J_2(L+1)$. (b) shows an additional row flipped. This has an energy of $8J_2$ higher than (a). (c) shows two additional rows flipped. (d) shows an edge being “eaten” away from both corners. Finally, (e) and (f) show two configurations not counted in our computation of the free-energy barrier. (e) is neglected because it is not a barrier configuration. Flipping the last spin the second row lowered the energy by $4J_2$. (f) is not included because spins are flipped in more than one layer. It is thus outside our approximation of considering only those barrier configurations in which just one layer is being peeled away from each corner.

Since the second lowest energy barrier is $8J_2$ higher than the lowest, using this expression for $\bar{\Gamma}_0$ introduces an error on the order of $e^{-8J_2/T}$ into our computation of t .

We will now present an approximate calculation for the free-energy barrier $F_B(T)$. Although the technique is similar to a low-temperature expansion for the equilibrium free energy, two points should be kept in mind. The first is that we want to include only “barrier configurations.” That is, for each path in configuration space, we are interested only in the configuration with the maximum energy along that path. Figures 4(a)–4(d) are examples of configurations that should be summed over, while Fig. 4(e) is an example of one that should not because a path in configuration space passing through such a configuration must first pass through a higher-energy configuration.

The second point is that we are not only interested in the thermodynamic limit ($L \rightarrow \infty$) because we wish to compare the resulting analytic expression to numerical data for quite small cubes. In Sec. II C, we will find that the expressions derived here simplify considerably in the thermodynamic limit. That limit is also much more forgiving: Many approximations (concerning which configurations to include) are irrelevant in the thermodynamic limit, but do make a significant difference for the cube sizes ($4 \leq L \leq 24$) in the Monte Carlo simulation.

Before proceeding with the calculation, let us summarize the approximations which will be made in computing F_B .

(1) We will work in the limit $J_1/J_2 \rightarrow \infty$. This is justified by the insensitivity of the simulation results to J_1/J_2 in the low-temperature region where our expression will be valid.

(2) We will allow only the spins in one layer of the cube to flip. Figure 4(f) shows an example of a neglected configuration. Since the number of neglected configurations is generally smaller (i.e., grows with a lower power of L) than the number of those with the same energy that are included, this should be a fairly benign approximation even for finite cubes. In the thermodynamic limit (and $J_1/J_2 \rightarrow \infty$), the free-energy barrier (per unit edge length) computed in this way becomes exact.

(3) We will enumerate the configurations approximately, e.g., by extending certain sums to infinity even though they would terminate for a finite cube. These again are the sorts of approximations which are irrelevant in the thermodynamic limit, but which can make a difference for finite cubes.

Finally, we remind the reader that in calculating the activation time t from F_B , we will approximate $\bar{\Gamma}_0$ as given by Eq. (2.9).

We proceed with the calculation as follows: First, we will consider only configurations where the edge is being “eaten away” from just one of the corners [i.e., neglecting configurations like Fig. 4(d), which have energies at least $8J_2$ higher than the configuration in Fig. 4(a)]. What we are then studying is simply the energies for various configurations of a step across the face of the cube.

These energies can easily be computed using the two rules given in Appendix B, which associate an energy with each plaquette (unit area) of interface and each bend in the interface. Since our approximations have reduced the model to a simple one-dimensional solid-on-solid (SOS) model, the energy of any configuration is specified by a series of non-negative integers m_i giving the difference in the step height between successive columns, as shown in Fig. 5. The energy associated with each such column is simply

$$E(m_i) = \begin{cases} 0 & \text{if } m_i = 0, \\ 4J_2(m_i + 1) & \text{if } m_i > 0. \end{cases} \quad (2.10)$$

If we ignore the finite length of the cube in the vertical direction, then we can allow each m_i to range over all non-negative integers (independent of each other). The partition function can thus be written as³¹

$$Z_B = e^{-4J_2(L+1)/T} (2Z_1^{L-2} - 1), \quad (2.11)$$

where Z_1 is the partition function for a single column:

$$Z_1 = \sum_{m=0}^{\infty} e^{-E(m)/T} = 1 + y, \quad (2.12)$$

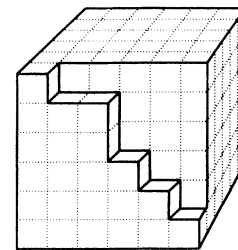
where

$$y \equiv \frac{e^{-8J_2/T}}{1 - e^{-4J_2/T}}. \quad (2.13)$$

The free-energy barrier (within the approximation that the edge is eaten away from only one of the corners) is then

$$F_B = 4J_2(L+1) - T \ln[2(1+y)^{L-2} - 1]. \quad (2.14)$$

If we now relax the assumption that the edge is eaten away from only one corner and, instead, allow it to be eaten away from both corners [as in Fig. 4(d)], the partition function can be written as



$$m_i = 0 \ 2 \ 1 \ 1$$

FIG. 5. Energies of configurations involved in approximating the free-energy barrier F_B . If we let m_i label the difference in the step height between successive columns, as shown, then the energy associated with the i th column is given by $E(m_i) = 4J_2(m_i + 1)$ for $m_i > 0$ and by $E(0) = 0$. (Of course, there will be an overall additional energy of $4J_2(L+1)$ from flipping the spins along the top row.)

$$Z_B = e^{-4J_2(L+1)/T} \left[(2Z_1^{L-2} - 1) + y \sum_{\mathcal{L}=0}^{L-3} (2Z_1^{\mathcal{L}} - 1)(2Z_1^{L-3-\mathcal{L}} - 1) \right]. \quad (2.15)$$

[Note that this *does* include the possibility that the two corners are peeling away two different faces, as occurs in Fig. 4(d) where the top face is peeling away from the right corner while the front face is peeling away from the left corner. Such configurations are important to count since they have the same energy as the corresponding configurations in which the same face is being peeled away from both corners.] Summing the geometric series, we obtain our final result:

$$F_B = 4J_2(L+1) - T \ln \{ 3 - 2(1+y)^{L-2} + (L-2)y[1 + 4(1+y)^{L-3}] \}, \quad (2.16)$$

where y is given by Eq. (2.13).

Equation (2.16) is our best approximation for the free-energy barrier to flip the first edge of a cubic droplet. Substituting this into Eq. (2.7) gives us the estimate of the

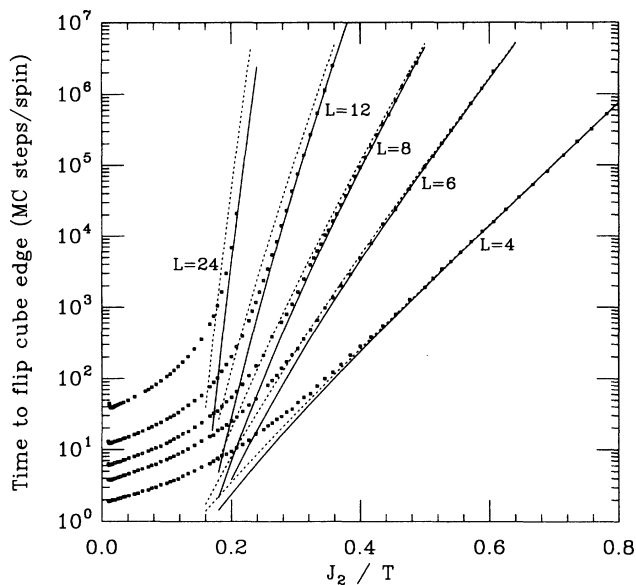


FIG. 6. The same simulation results as Fig. 3, but with improved theoretical forms. The solid curves are the theoretical form of Eq. (2.7) with Γ_0 given by Eq. (2.9) and the free-energy barrier F_B given by Eq. (2.16). The dotted curves use the cruder estimate for F_B given by Eq. (2.14), which does not include configurations where the edge is eaten from *both* corners. (In both cases there are no free parameters.) Note that in order to get essentially perfect agreement, it is necessary to include configurations in which the edge is “eaten” away from both corners, even though (as discussed in Sec. II C) such configurations do not change the expression for F_B/L in the thermodynamic limit $L \rightarrow \infty$.

time to flip the first edge of a cube, shown by the solid curves in Fig. 6. Clearly they are in excellent agreement with the Monte Carlo data at low temperatures.

C. The dynamical transition temperature

Now, we will take the thermodynamic limit $L \rightarrow \infty$ in order to calculate the free-energy barrier per unit edge length, f_B , to flipping the spins on an entire edge of a very large cube. At the temperature, T_{CR} , where $f_B \rightarrow 0$, the time to flip a cubic domain will no longer depend exponentially on its edge length. Thus, T_{CR} should mark the transition in the coarsening dynamics from logarithmic to $t^{1/2}$ coarsening. As will be explained in Sec. II D, the temperature T_{CR} we obtain is also precisely the temperature for an interfacial phase transition known as the corner-rounding transition (hence our use of the subscript “CR”).²⁷

In the thermodynamic limit, Eq. (2.16) simplifies considerably and the free-energy barrier per unit edge length becomes

$$f_B \equiv \lim_{L \rightarrow \infty} \frac{F_B}{L} = 4J_2 - T \ln \left[1 + \frac{e^{-8J_2/T}}{1 - e^{-4J_2/T}} \right]. \quad (2.17)$$

A plot of $f_B(T)$ is shown in Fig. 7. The temperature T_{CR} at which $f_B = 0$ is given by the cubic equation $x^3 - x^2 + 2x - 1 = 0$, where $x \equiv e^{-4J_2/T_{CR}}$. This cubic has one real root which yields the result

$$T_{CR} = \frac{-4J_2}{\ln(1/3 - 5/(9\beta^{1/3}) + \beta^{1/3})} \approx 7.1124 \cdots J_2, \quad (2.18)$$

where $\beta \equiv \frac{1}{6}(\frac{11}{9} + \sqrt{23/3})$.³² Since all the approximations we made in deriving f_B are irrelevant in the thermodynamic limit, our expression for the dynamical transition temperature should be exact in the limit $J_1/J_2 \rightarrow \infty$.

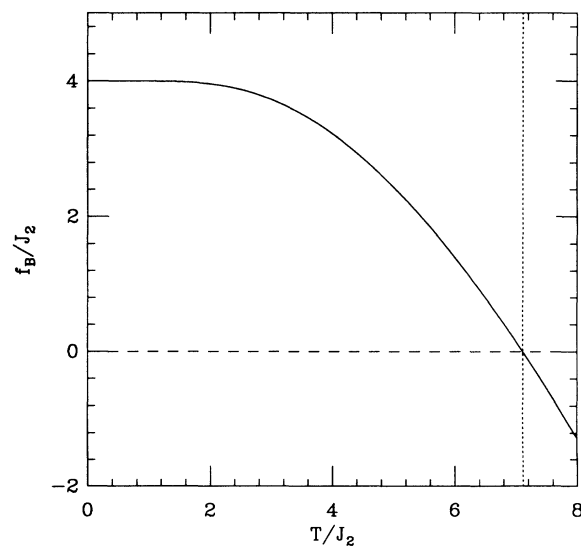


FIG. 7. The free-energy barrier per unit edge length, f_B , vs temperature T , as determined from Eq. (2.17). The temperature T_{CR} at which $f_B = 0$ is shown by a dotted line.

Finally, we might ask about corrections to T_{CR} for finite J_1/J_2 . Qualitatively, we expect T_{CR} will drop with decreasing J_1/J_2 and go to zero at $J_1/J_2=4$, where the ferromagnetic ground state becomes unstable. To obtain a good estimate for T_{CR} near $J_1/J_2=4$ would require including configurations involving multiple layers (see Ref. 29, Appendix B), and thus a much more concerted attack on the problem. We can, however, obtain an estimate of the importance of the corrections to our estimate of T_{CR} for finite J_1/J_2 by noting that they will come in with a factor like $e^{-4(J_1-4J_2)/T_{CR}}$. This suggests T_{CR} remains fairly close to its $J_1/J_2 \rightarrow \infty$ value until J_1/J_2 gets quite close to 4. For example, $J_1/J_2=12$ would yield a correction to T_{CR} on the order of 1% or less.

We have already made several allusions to the relation between the temperature at which the free-energy barrier per unit length goes to zero and an equilibrium interfacial transition known as the corner-rounding transition. In the following subsection, we will give a brief discussion of the interfacial phase transitions in this model and then finally make explicit the relationship between the coarsening dynamics and the corner-rounding transition.

D. Connection with equilibrium crystal shapes

The nearest-neighbor Ising model on a cubic lattice has a roughening transition at $T_R \approx 2.45J_1$.³³⁻³⁶ Below this transition, interfaces in equilibrium are macroscopically smooth in the sense that the variance of the fluctuations in the height of the interface remains bounded as the system size is taken to infinity. Above T_R , the interface is rough and the variance diverges as the logarithm of the system size.

The roughening transition can be thought of in two ways.³⁵ Macroscopically, it is the temperature at which the equilibrium crystal shape (ECS) loses its facets. That is, the ECS will have (macroscopically) flat [100] facets for $T < T_R$ and will be rounded for $T > T_R$. On a microscopic level, T_R is that temperature at which the step free energy for steps (of all orientations) across the [100] facet goes to zero. The step free energy is defined as the difference between the free energy per unit area for an interface with a step and the free energy per unit area of an interface without the step. (Note that it depends on *both* the orientation of the interface and the orientation of the step.³⁷) When this step free energy goes to zero, the interface roughens since there is no free-energy barrier to the creation of steps which can then proliferate without bound.

In the context of equilibrium crystal shapes, Rottman and Wortis^{27,38,39} have shown that the addition of NNN AFM bonds introduces two new transition temperatures which we will denote by T_{CR} and T_{ER} .⁴⁰ At temperatures $T < T_{CR}$, the ECS is a cube with macroscopically sharp edges and corners (see Fig. 8). Above the corner-rounding transition temperature, T_{CR} , the corners of the cube (or, equivalently, the edges near the corners) become rounded but at least part of the edge remains sharp. As the temperature is increased further, the rounding near the corners spreads out along the edges until, at T_{ER} , the

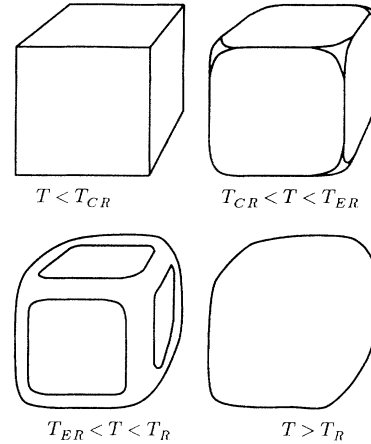


FIG. 8. Qualitative thermal evolution of the equilibrium crystal shape of the Ising model with weak next-nearest-neighbor antiferromagnetic bonds (after Ref. 27). For $T < T_{CR}$, the crystal has flat faces with macroscopically sharp edges and corners. Above T_{CR} , the crystal rounds near the corners; but up to a temperature of T_{ER} , at least part of the crystal edge remains sharp. Above T_{ER} , there are no sharp edges but there are still flat [100] faces. Finally, at the roughening temperature T_R , the crystal becomes completely rounded.

entire edge of the crystal is rounded. T_{ER} is thus referred to as the edge-rounding transition temperature.⁴¹ On the microscopic level, T_{CR} is defined as the temperature at which the step free energy, $f_{[111]}$, for a step across a [111] interface goes to zero. Analogously, T_{ER} is defined as the temperature at which the free energy, $f_{[110]}$, of a step across a [110] interface goes to zero.²⁹

Let us now consider how these transitions affect dynamics. The relation of the roughening transition to dynamics has been known since such a transition was first proposed. In fact, the interest in T_R was sparked by studies of crystal growth from the melt.³³ Below T_R , where growing crystals have smooth facets, the growth is quite slow. This is because the growth proceeds via the nucleation of a group of atoms (“islands”) on the surface. Such an island is only stable once a critical nucleus size has been reached, and thus a large free-energy barrier must be surmounted. Above T_R , when the surface is already rough, no such barrier exists.

We propose that the corner-rounding temperature T_{CR} marks a similar change in dynamical behavior: Below T_{CR} , there will be a free-energy barrier per unit length to depin a step from the edge of a domain, thus leading to logarithmically slow coarsening dynamics. How do we justify this claim that the dynamical transition temperature and the corner-rounding transition temperature coincide? The justification comes from the recognition that the free-energy barrier we calculated in Sec. II C is (up to a geometric factor⁴²) simply the step free energy, $f_{[111]}$, for a step across a [111] interface.⁴³ The result presented there [Eq. (2.18)] for the corner-rounding temperature T_{CR} is an exact expression in the $J_1/J_2 \rightarrow \infty$

limit. An alternative calculation of T_{CR} yielding precisely the same result has been given by Shi and Wortis.³⁸

III. NUMERICAL SIMULATIONS OF COARSENING

Before discussing the numerical simulations, it is worthwhile to reexamine our argument for logarithmic coarsening in more detail. In particular, we would like to explain why the argument based on shrinking cubic droplets may be more general than it first appears to be. The question to be addressed in this: Having identified one special configuration in which there are large barriers, why do we have reason to believe that such barriers will be present for the configurations which will occur during the coarsening process?⁴⁴

There are two points to be made in answering this question. First, an initial droplet which is not cubic will tend to shrink to a point where it has flat faces and sharp edges and then get stuck. We have confirmed this numerically by studying the time to shrink spherical droplets. The time it takes to shrink such a sphere of diameter D is in agreement with the expectation that the barrier is approximately determined by the largest cube contained inside the sphere, namely, one with edge length L close to (or a little less than) $D/\sqrt{3}$.

The second point is that the argument applies to a more general situation than merely the shrinking of isolated droplets. [This greater generality is necessary because isolated droplets (or, in the language of percolation theory, “clusters”), except of very small size, are a rare occurrence in the 3D Ising model. The reason is that the density of both up and down sites ($p=0.5$) is well above the percolation threshold ($p_c \approx 0.312$),⁴⁵ so the system consists primarily of two infinite clusters.] For example, a “handlelike” structure of size L on one of the infinite clusters should also have an energy barrier to shrinking which is proportional to L . We believe the fundamental point is that below T_{CR} there is a free-energy barrier per unit length to depin a step from an edge. This means that edges will tend to remain sharp and that the free-energy barriers to flip the spins along such an edge will diverge with the length of the edge. Since the length of edges in the system should be proportional to the characteristic length scale $L(t)$, we expect that the free-energy barriers will diverge with $L(t)$ and the growth of $L(t)$ will be logarithmic.

On the basis of these arguments and upon our numerical simulations of shrinking cubic droplets, we believe that the case for logarithmic coarsening is fairly strong. Ultimately, however, lacking a rigorous proof, we must turn to numerical simulations of the coarsening process in order to further test our hypothesis.

We study coarsening following an instantaneous quench from infinite temperature to a temperature $T < T_C$. Such a quench is implemented by starting with a random spin configuration at time $t=0$, and then evolving the system at temperature T , using Glauber single-spin-flip dynamics [Eq. (1.6)]. Further details of the Monte Carlo algorithm are given in Appendix C.

The most important quantity to monitor during coarsening is the characteristic length scale $L(t)$. In the

literature, many ways of measuring $L(t)$ are discussed.^{16,46} If scaling is obeyed, any physically reasonable measure of $L(t)$ should show the same behavior. (A discussion of the scaling of the correlation function is given in Appendix D.) We choose one of the most common and convenient measures of $L(t)$, which is to take $L(t)$ to be proportional to the inverse of the total perimeter of domain boundaries. [As is further elucidated in Appendix D, this corresponds to measuring the slope of the correlation function $C(r,t)$ near $r=0$.] That is, we define

$$L(t) \equiv \frac{-E_0^{NN}}{(E^{NN} - E_0^{NN})}, \quad (3.1)$$

where E^{NN} is the energy associated with nearest-neighbor bonds only and $E_0^{NN} \equiv -3NJ_1$ is this energy in the ground state.⁴⁷ The normalization of $L(t)$ is such that, on average, $L(t)=1$ for the random initial configuration.

Figure 9 shows the growth of $L(t)$ during coarsening in two dimensions. We see that for $J_2=0$, the simulation results obey the $t^{1/2}$ law quite well over the entire time. (There are some small, but statistically significant, deviations at early times.) Adding the NNN bonds changes the behavior in exactly the manner which we expect:

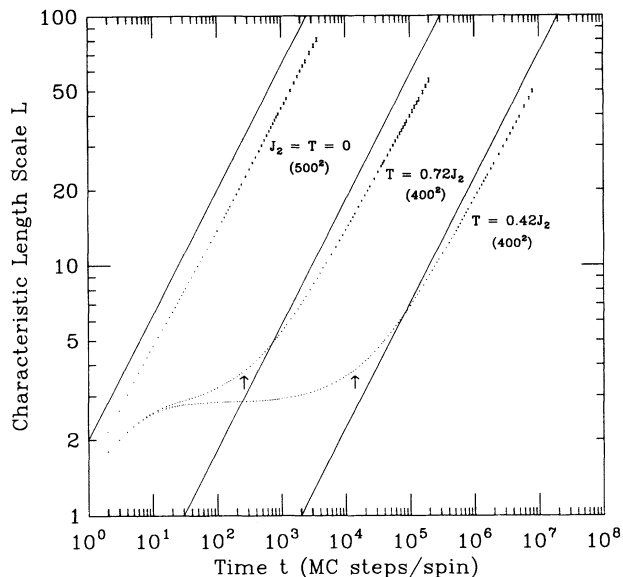


FIG. 9. Coarsening in two dimensions. This shows the growth of the characteristic length scale $L(t)$ for the 2D model following a quench from infinite temperature to the given temperature T . For the $J_2 \neq 0$ runs, we have chosen $J_1/J_2=6$. We have averaged over 30 or 40 runs with error bars showing the standard error. Numbers in parentheses give system sizes. (On this log-log plot, some straight lines of slope $\frac{1}{2}$ are shown to guide the eye.) For $J_2=0$, we see the expected $t^{1/2}$ growth law at all times. For $J_2 \neq 0$, the system initially coarsens on very short length scales, but then gets stuck. Little further coarsening occurs on time scales shorter than $t = e^{4J_2/T}$ (marked by arrows). However, if we look at the coarsening on time scales greater than this, the energy barriers can be crossed and the length scale grows as $t^{1/2}$.

After a short period of relaxation on the shortest length scales, the system finds itself in a configuration in which it must flip corners to coarsen further. Since the energy barrier to flip such a corner is $4J_2$, the system is stuck and coarsens little on time scales $t \ll e^{4J_2/T}$. However, at a time of order $e^{4J_2/T}$, we see a dramatic upturn on this log-log plot. This is because on time scales $t \gg e^{4J_2/T}$, the energy barriers can be crossed and we see $t^{1/2}$ behavior. This confirms our prediction that the 2D model is a class-2 system.³

Now let us consider Fig. 10 which shows the growth of the characteristic length scale in three dimensions. As in two dimensions, there is a short period of fast relaxation on very short length scales. After that, there is a period in which the growth is roughly a power law $t^{n_{\text{eff}}}$ with the effective exponent n_{eff} for the domain growth (given by the slope on this log-log plot) ranging from 0 (total freezing) for $T/J_2 \rightarrow 0$, to ~ 0.35 for $J_2=0$. For $T=2, 3$, and $4J_2$, there is considerable downward curvature in the data at late times, suggesting a crossover to logarithmic growth. No such downward curvature is evident for $J_2=0$ or for $T=8J_2$ (which is above the corner-rounding temperature T_{CR}) until finite-size effects lead to a quite sharp flattening out once $L(t)$ is roughly a third the system size.

Two brief comments are in order. First, let us consider the behavior for $J_2=T=0$: The data appear to obey a

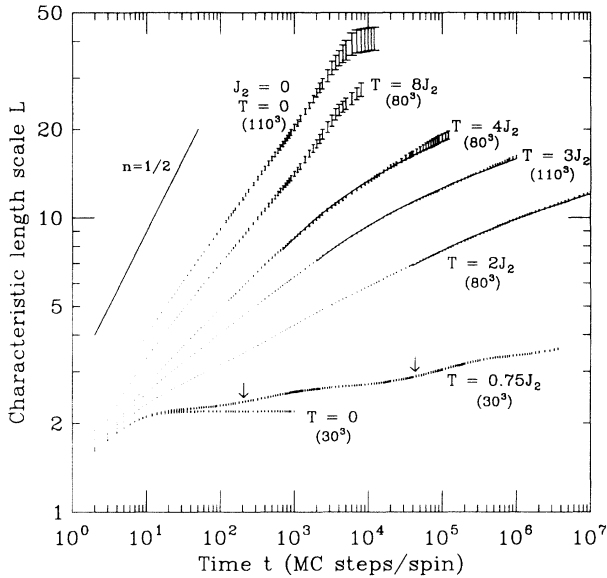


FIG. 10. Coarsening in three dimensions. This shows the growth of the characteristic length scale $L(t)$ for the 3D model following a quench from infinite temperature. Each set of Monte Carlo data is from an average over 10–20 runs with error bars giving the standard error. (The scatter in the data is much less than the error bars would suggest because the error is strongly correlated in time.) For $T=8J_2$, we have chosen $J_1/J_2=50$, while for the rest (excluding $J_2=0$, of course), $J_1/J_2=6$. For $T=2, 3$, and $4J_2$, the solid curves show two-parameter fits at late times (over the interval for which the curve is shown) to the form $L(t)=a \ln(t/t_0)$. Arrows for $T=0.75J_2$ indicate the times at which $t=e^{4J_2/T}$ and $t=e^{8J_2/T}$.

power law quite well over a full two decades in time and yet the power is found to be about 0.35, much closer to $\frac{1}{3}$ than to $\frac{1}{2}$. This is a surprising result since it is gospel that the nearest-neighbor Ising model obeys the Lifshitz-Allen-Cahn law. This anomalous exponent is discussed in more detail elsewhere.²⁹ Here, it will suffice to say that similar behavior (an exponent of ~ 0.37) has been seen by Amar and Family,⁴⁸ in the only other study (as far as we know) of coarsening in the 3D Ising model at zero temperature. Since some of their calculations were performed on very large (512^3) systems, we can be confident that this is not a finite-size effect. On the other hand, we cannot rule out the possibility that this is simply a very long-lived transient. This may indeed be the case, but there exists the intriguing possibility that there is truly a different exponent (or a breakdown of scaling altogether^{29,48}) at $T=0$. (The numerical evidence suggests that the $t^{1/2}$ law will be obeyed at late enough times for any nonzero temperature.²⁹)

A second comment concerns the interesting behavior seen for $T=0.75J_2$, where there are clearly steps in the data. These steps are indicative of the discreteness of the energy barriers in our system. On time scales $t \ll e^{4J_2/T}$, any spin flips which raise the energy are unlikely to occur. Then, on time scales $e^{4J_2/T} \ll t \ll e^{8J_2/T}$, energy barriers of $4J_2$ are crossed regularly, but those of $8J_2$ are not, and so on. The origin of these steps is thus the same as that which leads to the change in behavior in the 2D model at a time of order $e^{4J_2/T}$, except that here there is more than one barrier height present in the coarsening system. For quenches to somewhat higher temperatures, the steps are closer together. By a temperature of $T=2J_2$, they have been washed out.

Now let us look more closely at the data for moderate values of T/J_2 . One could conclude from these results that at long times there will be power-law behavior with the exponent itself a continuous function of the ratio T/J_2 . However, even neglecting the considerable downward curvature at late times, this scenario seems rather unlikely to us (although certainly not forbidden) since we know of no proposals that a coarsening system will have a continuous set of exponents, $n(T)$. A more likely explanation is that this is a transient behavior and that at longer times there will either be upward curvature with a return to $t^{1/2}$ behavior (as occurs in the 2D model) or slow downward curvature compatible with our prediction of logarithmic growth. Apparent power-law growth with temperature-dependent effective exponents has commonly been seen in Monte Carlo simulations of systems which freeze at zero temperature. It occurs both in systems which are known to obey $t^{1/2}$ or $t^{1/3}$ growth laws^{3,49} at long times and those believed to obey logarithmic growth laws.⁵⁰

A. Evidence for logarithmic growth of $L(t)$

We now ask whether the data in Fig. 10 is more compatible with a return to $t^{1/2}$ behavior or with a logarithm. There are several reasons why we prefer the latter explanation. First, one can estimate the largest barrier

heights involved in the coarsening process out to the times studied by noting that at $t = 10^6$ MC steps/spin and $T = 3J_2$, the time is 3 orders of magnitude larger than the time taken for equivalent coarsening in a system with $J_2 = 0$. From this, we can get an estimate of the energy barriers E which are being crossed by setting this ratio of time scales equal to $e^{E/T}$; this gives $E \approx 20J_2$. Activation over such large barriers suggests a process involving the cooperative flipping of several spins. In addition, as long as the data for $J_2 \neq 0$ has a smaller slope than that for $J_2 = 0$, this difference in time scales (and the energy barriers it implies) will continue to grow.

There are two caveats which must be noted. First, the barrier of $20J_2$ is that associated with flipping an edge of length 4, while $L(t)$ is about three times this large. We believe this discrepancy is due to the fact that $L(t)$ gives only an average length scale in the system, whereas the active processes will be determined by the shortest length since these will be the fastest. That there are a distribution of lengths in the system is apparent when we look at the spin configurations during the coarsening.

The second caveat is that there is, of course, a larger energy scale than J_2 in our system, namely, J_1 . Our simulations do not go out far enough in time to rule out the possibility that at long times the system can avoid the growing J_2 barriers by going over large, but L -independent, J_1 barriers. We cannot envision such a scenario, but have not *proven* its impossibility. In order to test the sensitivity of our results to J_1 , we increased the ratio of J_1/J_2 and find that the results change only a little (with the downward curvature becoming slightly more pronounced). This suggests that activation over J_2 — and not J_1 —barriers is what is important here. Nonetheless, not being able to carry out our simulations to times which are much greater than any single-spin J_1 barriers in our problem is probably the greatest weakness in the conclusiveness of the numerical results. Ultimately, the best evidence that J_1 is not relevant will be provided in Sec. IV, where we introduce the tiling model. In that model, the energy scale J_1 is eliminated altogether in a natural way by incorporating it into a constraint on the dynamics.

Now to the second, and primary, reason for believing the growth to be logarithmic: the downward curvature apparent in the data at late times for $T = 2, 3$, and $4J_2$. It suggests that, as the shortest lengths in the system become large enough for our arguments to apply, there is a crossover to slower growth. In order to test whether the growth is, in fact, becoming logarithmic, we show two-parameter fits to the form $L(t) = a \ln(t/t_0)$ over the last two to three decades in time. There is evidence of some systematic disagreement (with the Monte Carlo data having less curvature than the fits), but, in general, the fits are quite good, and are far superior to any straight-line (i.e., power-law) fits. (Why is there still some systematic deviation from logarithmic behavior at these latest times? In part this may be evidence that we are still not yet quite in the late-time, scaling regime; but some of the deviations may be accounted for by the fact that in this scaling regime we would really expect the length scale to satisfy a

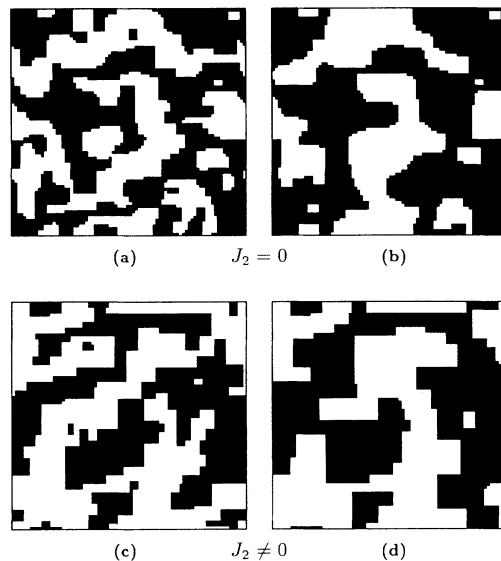


FIG. 11. A comparison of the spin configurations in one layer (a slice) of an 80^3 coarsening system for $J_2 = 0$ and $J_2 \neq 0$. (a) and (b) show configurations for $J_2 = 0$, while (c) and (d) show configurations for $T = 3J_2$. Spin up and spin down are denoted by solid and open squares, respectively. The times have been chosen so that $L(t)$ is approximately equal to 6.3 in (a) and (c), and to 9.5 in (b) and (d). As expected, the configurations for $J_2 \neq 0$ show a much stronger preference for flat boundaries aligned along the lattice directions.

differential equation of the form

$$\frac{dL}{dt} \sim \frac{e^{-f_B L/T}}{L}. \quad (3.2)$$

That is, we must include the $1/L$ curvature force term. This equation only asymptotically gives the form $L(t) = a \ln(t/t_0)$. Indeed, we find that fits over the same range of times to the full form obtained from integrating Eq. (3.2) are better than the fits shown, having virtually no systematic deviation.⁵¹⁾

The final reason for believing the long-time growth to be logarithmic comes from observing the spin configurations which occur during a quench. Figure 11 compares a 2D slice through a system with $J_2 = 0$ to that with $J_2 \neq 0$, at two times during the coarsening. In contrast to spin configurations for the unfrustrated ($J_2 = 0$) model, the configurations for $J_2 \neq 0$ are clearly “blocky,” with a strong preference for flat faces aligned along the simple-cubic directions. Thus, the system seems to be getting stuck in the sort of configurations where our argument for logarithmic growth should hold.⁵²⁾

B. Tests for finite-size effects

We will now briefly consider another possible source of the downward curvature seen in Fig. 10 for $T = 2, 3$, and $4J_2$: finite-size effects. It is apparent from the data for $J_2 = 0$ and $T = 8J_2$ that the effect of the periodic boundary conditions is to introduce downward curvature once $L(t)$ gets large. However, this curvature is qualitatively

different than what we see for $T=2, 3$, and $4J_2$. It is quite sharp rather than gradual, and, as a result, it cannot be fit to a logarithmic form over any reasonable range of times.²⁹ Furthermore, it occurs at a considerably larger value of L . [In particular, compare $J_2=0$ to $T=3J_2$, where both runs are on $(110)^3$ systems.] Nonetheless, the possibility that the curvature could be due to finite-size effects is certainly worth investigating more closely.

Why do periodic boundary conditions produce a cutoff in the growth of $L(t)$? This cutoff is due to the development of flat slabs and tubes extending the entire length of the system (and thus, in a sense, infinite), as has been discussed by others.⁵³ These configurations are metastable since there are barriers of at least $4J_1$ to flipping any spins. Because we are studying this model at temperatures $T \ll 4J_1$, these metastable states are very long lived. Furthermore, they are much more common in three dimensions than in two, since the fraction of each type of spin, $p=0.5$, is far above the percolation threshold for three dimensions but coincides with it for two dimensions.

We have studied the finite-size effects in two ways. First, we have tried changing the boundary conditions from periodic to antiperiodic (in all three lattice directions). This has the effect of forcing an interface in the system and thus should rid us of the slab and tube effects. (Of course, such boundary conditions presumably introduce some of their own idiosyncrasies—we do not claim these boundary conditions are better, but only that they are different. In particular, since an interface is forced in the system, the largest possible value that L [as defined by Eq. (3.1)] can assume in an \mathcal{L}^3 system is $\mathcal{L}/2$,⁵⁴ so there will still be a cutoff in L due to finite-size effects.) With these boundary conditions, there is no detectable change in the curvature for $T=3J_2$. Second, we have investigated the effect of varying the system size. We have done this most systematically for $T=3J_2$, where we find that there seems to be no statistically significant difference between a 110^3 and an 80^3 system, out to at least $t=10^5$ MC steps/spin. For a 55^3 system (where the run-to-run variation at late times is quite large and the results correspondingly less trustworthy), the data have a tendency to have a bit *less* curvature than for the runs at larger system sizes. On the basis of these tests, we conclude that it is extremely unlikely that the downward curvature in Fig. 10 for $T=2, 3$, and $4J_2$ is due to finite-size effects.

IV. THE TILING MODEL

A. Introduction to the tiling model: statics

In this section, we study the dynamics of what we dub the “tiling model.”^{38,55,56} This is a 2D model for a [111] interface in our 3D model. A sample configuration of this model is shown in Fig. 12. The model views the interface from the [111] direction, which means that we are seeing a corner between the [100], [010], and [001] facets head on.

In the statistical mechanics literature, this model is known as the [111] restricted solid-on-solid ([111]-RSOS) model. “Restricted” here refers to the fact that in this

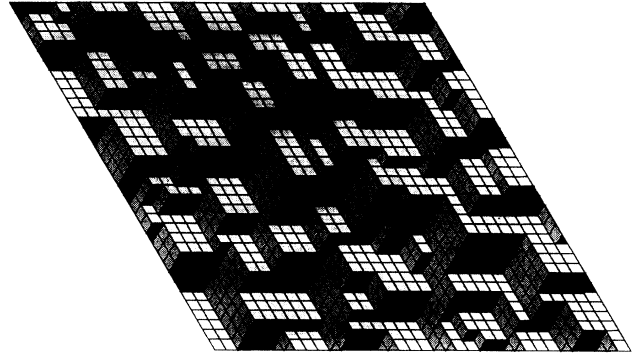


FIG. 12. A sample configuration for the tiling model. Viewed from the [111] direction, an interface in a 3D model can be represented by a tiling of the plane by rhombi of three orientations, provided that the interface has no overhangs when thus viewed. (We have shaded the three types of rhombi differently in order to distinguish them more easily and enhance the 3D perspective.) If we assign an energy of $2J_2$ to each unit length of boundary between the different types of tiles, then the energetics of this model matches that of the 3D Ising model with next-nearest-neighbor antiferromagnetic bonds.

model interface configurations are restricted to those in which the entire interface is visible when viewed from the [111] direction. (That is, configurations with “overhangs,” an example of which is shown in Fig. 13, are forbidden.) It is the absence of overhangs which allows the interface to be represented by a tiling of the plane with 60° rhombi of three different orientations.⁵⁷ To make the energies of the tiling configurations correspond to those of an interface in our 3D model with AFM NNN bond strength J_2 , we assign an energy of $2J_2$ for each unit length of boundary between unlike tiles.⁵⁸ Note that since the RSOS restriction forces the interfacial area to remain constant, the tiling model corresponds to the limit $J_1 \rightarrow \infty$ in the 3D model.

At low temperatures, we expect the tiles to phase separate, representing the fact that only a sharp corner in the 3D model is thermodynamically stable. At high temperatures, the different types of tiles should intermingle to form a thermodynamically rough [111] interface. Clearly the phase transition in the tiling model will occur at the point where the sharp corner rounds, i.e., at the corner-rounding transition T_{CR} of the 3D model. In fact, following the introduction of a related model by Blöte and Hilhorst,⁵⁵ the tiling model was used by Shi and Wortis³⁸ to study the corner-rounding transition of a

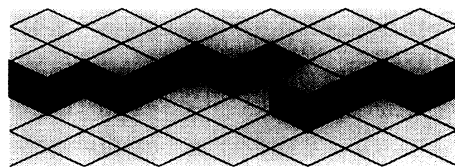


FIG. 13. An example of an interface configuration which cannot be represented by the tiling model. Part of the interface is hidden from view (i.e., there is an “overhang”) and this results in some incomplete (triangular) tiles.

sodium chloride (NaCl) crystal in equilibrium with its vapor. Much of our introductory discussion here follows closely that in Ref. 38.

An important feature to notice about this model (which is also true of other restricted solid-on-solid models⁵⁹) is that excitations can only occur along the boundary between the domains.⁶⁰ Below T_{CR} , three “frozen phases” coexist, corresponding to the microscopically flat [100], [010], and [001] facets; the entropy per tile is zero in the thermodynamic limit. Of course, in any finite system, there will be thermal excitations along the boundaries between domains.

We have explained how the tiling model is viewed either as a 2D tiling of the plane by rhombi or as the projection of an interface in three dimensions. Before discussing the dynamics of this model, we will briefly discuss a third representation^{38,55} (which is useful for implementing the dynamics): an Ising spin system on a triangular lattice. The mapping from a tiling configuration to the corresponding spin configuration, examples of which are shown in Fig. 14, is made by placing a spin at each vertex such that the spins are antiferromagnetically aligned along the edges of the rhombi. The mapping is unique up to an overall inversion of the spins.

Any spin configuration produced by a perfect tiling has, for each elementary triangle, two out of three spins aligned. Thus, the correspondence is between tilings and ground-state configurations of the NN AFM Ising model on a triangular lattice. The energetics of the tiling and the corresponding spin configuration is reproduced if we choose J_2 to be the bond strength for AFM NNN bonds between the spins. Thus, the tiling model with an energy cost of $2J_2$ per unit length of domain boundary can be represented by the following Ising Hamiltonian on a triangular lattice:

$$H = J_1 \sum_{NN} s_i s_j + J_2 \sum_{NNN} s_i s_j, \quad (4.1)$$

with $J_1 \rightarrow \infty$, $J_2 > 0$, and $s_i = -1$ or $+1$. Since the spin configurations of (4.1) are far less compelling visually than the corresponding tilings, particularly in making the connection with our 3D model, we will make only occasional reference to this representation from here on.

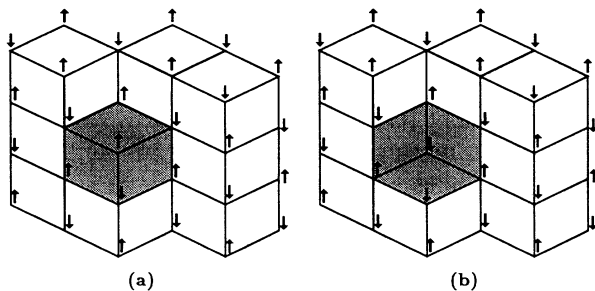


FIG. 14. The elementary dynamical move in the tiling model. In the 2D spin representation, the move consists of flipping a spin which has exactly three of its six nearest neighbors aligned. In tiling language, it consists of a rotation of an elementary hexagon (shaded) by 60° . From a 3D perspective, we see that it represents an elementary cube either added or taken away.

However, it is the representation which is computationally the most convenient in performing the Monte Carlo simulations.

B. Dynamics

We will use Glauber single-spin-flip dynamics [Eq. (1.6)] on the spins of Eq. (4.1). Since we are in the $J_1 \rightarrow \infty$ limit, the only spins that can flip are those which have three of their six nearest-neighbors aligned. In tiling language, such a spin-flip corresponds to rotating an elementary hexagon consisting of three tiles, as shown in Fig. 14. Finally, in the original 3D Ising description, it corresponds to adding or removing an elementary cube (i.e., to flipping the spin that this cube represents).

From Fig. 12, we see that there are relatively few such elementary hexagons, and thus few sites where this dynamical move can take place. This is, of course, a consequence of the RSOS restriction (or, in terms of the corresponding 3D model, because we are in the limit $J_1 \rightarrow \infty$).

It is important to note that, even though this model represents an interface of the 3D model, when we study coarsening in the two systems we are looking at different processes. In the 3D model, we studied coarsening for an entire 3D system, not just a single interface. In particular, we were interested in the decrease in the total interfacial area over time. It was the inverse of this total area which gave us our characteristic length scale.

Here, by contrast, we are confining ourselves to one particular interface of a *fixed* area. Rather than studying how the total interfacial area shrinks, we are instead concerned with how the structure of this one interface itself coarsens. To that end, we will quench the system from a temperature where the [111] interface is thermodynamically stable in the rough phase to a temperature where it is unstable and thus reconstructs into pieces of [100], [010], and [001] facets.⁶¹ We then look at the coarseness of this reconstructing interface over time.

In the 3D model, the order parameter was not conserved by the dynamics, and the naively expected power law was $L(t) \sim t^{1/2}$. However, because the coarsening involved activation over barriers that grow with $L(t)$, logarithmic growth was found to occur. In the tiling model, the order parameter (measuring the local tile orientation) is conserved by the dynamics, as can be seen from Fig. 14, and thus the naively expected power law is now $L(t) \sim t^{1/3}$. However, the method by which the interface coarsens involves activation over precisely the same sort of energy barriers as in the 3D model, and thus the same arguments we made for logarithmically slow coarsening in that model will apply here as well.⁶²

Although the tiling model is a bit more obscure than the Ising model on a cubic lattice, it has several advantages over our 3D model, upon which we now elaborate.

(1) Since the tiling model is two dimensional, the configurations are considerably simpler and easier to visualize. Furthermore, since there are three types of tiles, each has a density of $p = \frac{1}{3}$, which is well below the percolation threshold. As a result, the domains are compact, with structures much closer in form to cubical pro-

jections⁶² than the convoluted domains in our 3D model are to cubes.

(2) The simulations in 3D go out far enough in time to show that the system should be crossing energy barriers which are large in comparison to $12J_2$, the largest J_2 energy cost for flipping a single spin. However, the times are not long enough that single-spin-flip barriers of 8 or $12J_1$ are being crossed. Thus, the simulations themselves do not exclude the possibility that, once barriers of 8 or $12J_1$ could be crossed, the system would get “unstuck” and coarsen like $t^{1/2}$. Therefore, strictly speaking, our numerical work really only proves the claim of logarithmic coarsening in the limit of $J_1 \rightarrow \infty$. Since this limit corresponds to $T_C \rightarrow \infty$, our numerical work is most definitive in the singular limit $T/T_C \rightarrow 0$. The tiling model eliminates the possibility of activation over J_1 barriers by replacing the energy scale J_1 entirely by a constraint on the dynamics. Admittedly this constraint is equivalent to the limit $J_1 \rightarrow \infty$, but such a limit does not seem unreasonable since the order-disorder transition, T_{CR} , in this model is proportional to J_2 , not J_1 . Thus, our argument for logarithmic coarsening can be tested numerically over a large interval of T/T_{CR} . (We expect it to hold all the way up to the transition.)

(3) Finally, one might imagine that by eliminating one spatial dimension, we should be able to get even more convincing numerical results with the available amount of computing power. In fact, we will see that this does not appear to be the case. As with the 3D model, the slow dynamics which we are studying also slows the approach to the scaling regime where $L(t)$ assumes its asymptotic behavior. Nonetheless, we feel the numerical evidence is compelling enough that it would truly be perverse if $L(t)$ resumes the naively expected $t^{1/3}$ growth at times beyond the longest times we reach in these simulations.

C. Simulations of coarsening in the tiling model

We study the coarsening following a quench from infinite temperature (i.e., a random tiling) to a final temperature T .⁶³ Once again, we take the characteristic length scale $L(t)$ to be inversely proportional to the total perimeter of boundary between the domains. In particular, we define

$$L(t) \equiv \frac{-2.5E_0}{E - E_0}, \quad (4.2)$$

where E is the energy, and $E_0 \equiv -NJ_2$ is the energy of the ground state (i.e., where the total perimeter of domain boundaries is zero⁶⁴). The arbitrary constant 2.5 is chosen for convenience so that $L \approx 1.0$ for the initial random tiling.

1. Configurations during coarsening

Before studying the growth of $L(t)$ in quantitative detail, let us first discuss the qualitative features of the configurations as they evolve over time. Figure 15 shows the evolution of the domain structure following a quench to $T=3J_2$. We see the expected sharp boundaries be-

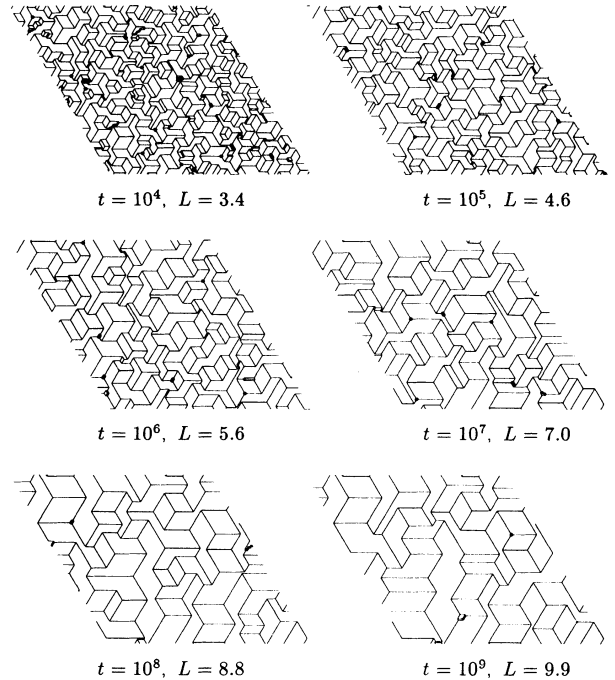


FIG. 15. Snapshots of the coarsening of the tiling model at various times t (measured in MC steps/spin) following a quench from infinite temperature to $T=3J_2$. This system has 120^2 sites. Only the boundaries between domains of equally oriented tiles are shown.

tween domains. As the length of these sharp edges increases, the energy barriers which must be surmounted to further coarsen the system should increase.

One might argue that there has been significant coarsening of the domain structure over the time period shown. However, it is important to notice the large range of time scales over which these snapshots have been taken. If the system were coarsening like $L(t) \sim t^{1/3}$, then the characteristic length scale would have grown by a factor of almost 50 between $t = 10^4$ and $t = 10^9$ MC steps/spin. Instead, it has grown by only a factor of 3.

In addition to studying still snapshots like these, we have also made an animated “movie” of the evolution of the system. Such a movie shows compellingly the effect of the large activation barriers. At late times, the system spends nearly all of its time “climbing” part of the way up these barriers (e.g., flipping a few spins along the edge of a domain) and then falling back down to its original state. Only rarely does it succeed in surmounting the barriers and finding a lower energy state.

2. Growth of the characteristic length scale

Now we will examine the growth of $L(t)$ quantitatively. Figure 16 is a log-log plot showing the growth of the characteristic length scale over time. We see the same basic trend that we saw for the 3D model (cf. Fig. 10). At the lowest temperatures, we see the steplike behavior in

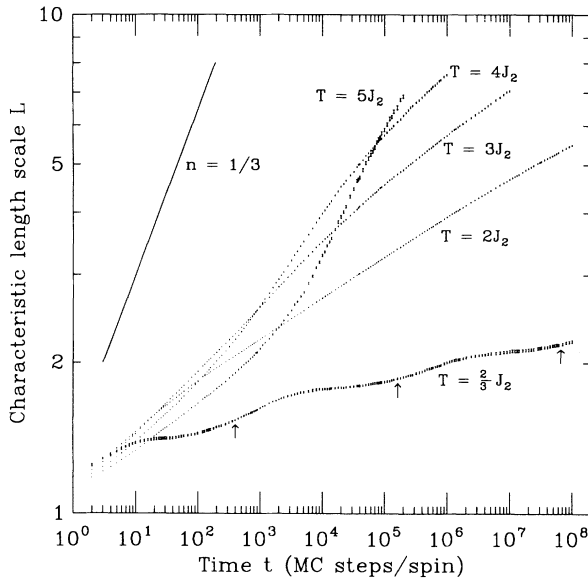


FIG. 16. Coarsening in the tiling model. This log-log plot shows the growth of the characteristic length scale $L(t)$ for the tiling model following a quench from infinite temperature. For $T = \frac{2}{3}J_2$, we study a 60^2 system and average over 12 runs. For the others we study a 120^2 system and average over 89–170 runs. Arrows for $T = \frac{2}{3}J_2$ indicate the times at which $t = e^{4J_2/T}$, $e^{8J_2/T}$, and $e^{12J_2/T}$. The solid line has a slope of $\frac{1}{3}$.

$L(t)$ which occurs as the system reaches time scales when it is first able to surmount barriers of height $4J_2$, then $8J_2$, and then $12J_2$. For higher T/J_2 , these steps get washed out and the effective exponent n_{eff} (the slope on this plot), increases toward $\frac{1}{3}$. For a given value of T/J_2 , n_{eff} appears to be slowly decreasing over time at late times. [For $T = 4J_2$ and especially for $T = 5J_2$, n_{eff} is lower than for $T = 3J_2$ at early times, but then increases at moderate times before appearing to decrease again at late times. The behavior at early and moderate times is a result of the sensitivity of our measurement of $L(t)$ to thermal fluctuations along the domain boundaries. This will be discussed further in Sec. IV C 3.]

The most sensitive test of whether the growth of $L(t)$ is becoming logarithmic at late times is to study a plot of the slope, $dL/d[\ln(t)]$, of the Monte Carlo data when shown on a log-normal scale. On such a plot, an approach to logarithmic growth would be indicated by having $dL/d[\ln(t)]$ level off, i.e., become constant, at late times. Such a plot (see Ref. 29, Fig. 4.12) shows that the slope appears to be leveling off only a little for $T = 2J_2$ and $T = 3J_2$. For $T = 4J_2$, the slope is leveling off more dramatically; however, since thermal fluctuations are quite important at $T = 4J_2$ even out to quite long times (as discussed in Sec. IV C 3), this result should be regarded with a bit of skepticism. We must conclude that out to the times studied in Fig. 16 we have not yet reached the time regime when the growth is clearly logarithmic.

In order to better determine the long-time behavior of $L(t)$, we have carried out a few individual runs to times

as long as $t = 2 \times 10^9$ MC steps/spin. The results are presented in Fig. 17. Also shown are logarithmic and power-law fits to the Monte Carlo data of Fig. 16 over the final decade in time ($t = 10^6 - 10^7$ MC steps/spin for $T = 3J_2$, and $t = 10^5 - 10^6$ MC steps/spin for $T = 4J_2$). Since there are large run-to-run fluctuations, it is hard to come to any firm conclusions. However, the data generally seem to lie between the logarithmic and power-law extrapolations. This suggests that although the data still are not quite fit by a logarithm, the exponent for the power-law fit (which is already very small) is continuing to decrease. This gives us confidence that the growth at asymptotically long times will, in fact, be logarithmic (or at least slower than power law). Unfortunately, the same barriers which produce this slow growth appear, not surprisingly, to slow the approach to this asymptotic behavior.

In order to show that the free-energy barriers to coarsening at these late times clearly involve the flipping of many spins, we estimate a lower bound for these barriers as follows: We consider the form $L(t) = a(t/\tau)^{1/3}$ with $\tau = \exp(F_B/T)$ and a of order 1. (In effect, we are asking the question, “If $L(t)$ resumed a growth law of $t^{1/3}$ at times just after we stopped our simulations, then what would we conclude were the heights of the largest free-energy barriers which the system had to cross during the coarsening process?”) Using the Monte Carlo data at the longest times gives $F_B \approx 40J_2$ and $55J_2$, for $T = 3J_2$ and $4J_2$, respectively (which is roughly the barrier heights we would expect given the values of L). By com-

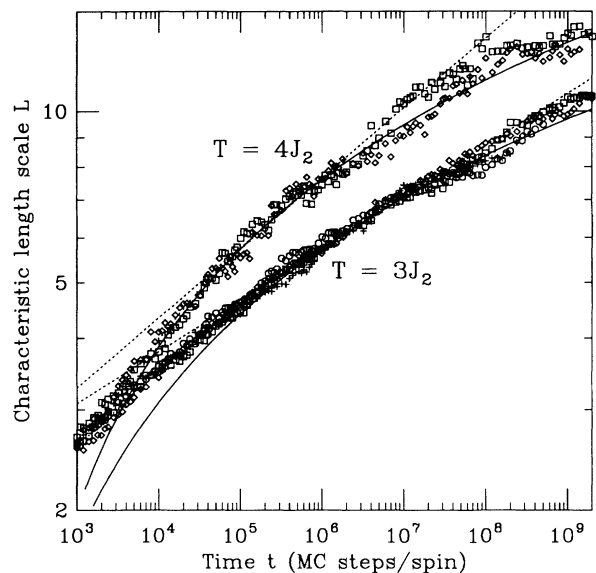


FIG. 17. Coarsening in tiling model: Long times. Here we show the growth of $L(t)$ for two runs at $T = 4J_2$ and four runs at $T = 3J_2$ which go out to very long times. The solid lines are fits to the logarithmic form $L(t) = a \ln(t/t_0)$ using the last decade of the Monte Carlo data in Fig. 16 ($t = 10^6 - 10^7$ MC steps/spin for $T = 3J_2$, and $t = 10^5 - 10^6$ MC steps/spin for $T = 4J_2$). The dotted lines are fits to the power-law form $L(t) = at^n$ using the same data. (The value obtained for the exponent n is 0.09 for $T = 3J_2$, and 0.12 for $T = 4J_2$.)

parison, the energy barrier to flip any single spin in this model is *at most* $12J_2$, and the barrier per unit length of edge is only $4J_2$.

3. Effects of thermal fluctuations and finite system size

In Sec. IV C 2, we noted that $T=4J_2$ and $5J_2$ (and for $T=3J_2$ at very early times), there is some upward curvature in Fig. 16 at short and intermediate times. The reason for this is that when domains sizes are small, the thermal fluctuations along the domain boundaries lengthen the total perimeter significantly and thus decrease the characteristic length scale $L(t)$ as measured by the inverse of this total perimeter [Eq. (4.2)]. This can be seen clearly in Fig. 18.

We have tried to correct for these thermal fluctuations by measuring $L(t)$ only after first quenching the system to $T=0$, or by using different measures of $L(t)$ which we hoped would be less sensitive to the thermal fluctuations,⁶⁵ but none of these methods were completely effective.²⁹ Since we have not yet found an adequate way to correct for thermal fluctuation effects, we must ask to

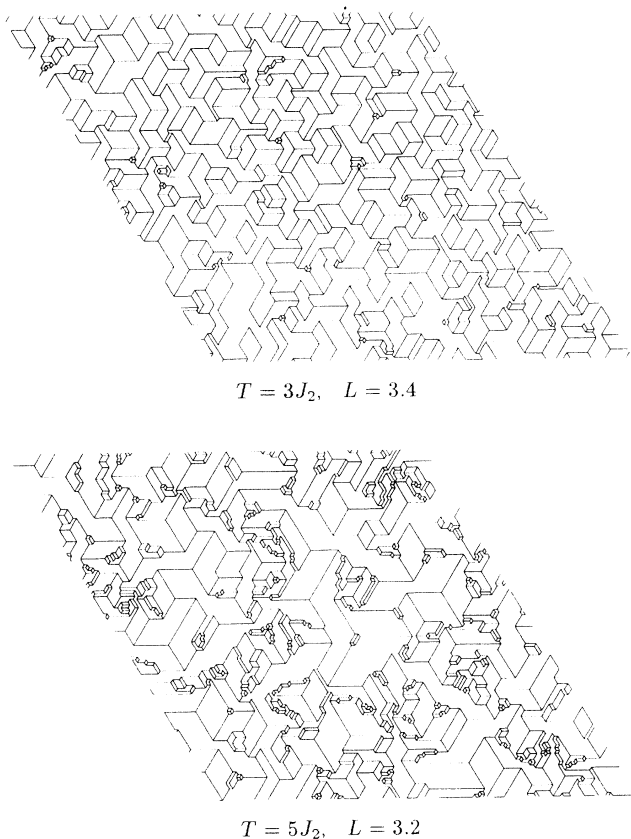


FIG. 18. Snapshots of the tiling model (system size = 120^2) as it coarsens for $T=3J_2$ and $5J_2$, both at $t=10^4$ MC steps/spin. The boundaries between domains are shown. Due to the thermal fluctuations along the boundaries, the length scale L as measured by Eq. (4.2) is slightly smaller for $T=5J_2$ than for $T=3J_2$, even though the system at $T=5J_2$ is clearly considerably coarser.

what extent they make our measurement for $L(t)$ untrustworthy. Fortunately, since the fluctuations occur only along the domain boundaries, the error in the measured length scale should decrease as the domain sizes grow. From Fig. 15, our study of alternate definitions of $L(t)$, and our studies of measuring $L(t)$ after quenching to $T=0$, we conclude that the data for $T=3J_2$ should be trustworthy at least for times $t > 10^5$ MC steps/spin. For $T=4J_2$ and $T=5J_2$, the situation is more unclear. However, even the $T=4J_2$ results are probably quite trustworthy at the latest times.

Finally, a few words on finite-size effects. To test for finite-size effects, we have run simulations for $T=3J_2$ on a system of half the linear size (60^2). A comparison of the results to those shown in Fig. 16 shows no evidence of any systematic deviation. The Monte Carlo data for the two systems agree within the (quite small) error bars. Since even the 60^2 system shows no evidence of finite-size effects out to at least $L \approx 7$, we imagine the results on 120^2 systems should be trustworthy out to at least $L \approx 14$. Thus, all the results we have presented should not have any significant finite-size effects.

D. Growth of order during slow cooling

In our 3D model, there are two distinct temperatures. One is T_C , below which ordering occurs. The other is T_{CR} , below which free-energy barriers are proportional to the length scale, thus slowing the dynamics. Since $T_{CR} < T_C$, this model orders without difficulty if it is cooled slowly. It must be *quenched* from $T > T_C$ to $T < T_{CR}$ in order to exhibit the logarithmically slow growth of order.

However, in the tiling model the ordering temperature and the temperature for slow dynamics coincide. Naively, we might hope that such a model will truly behave like a glass in the sense of having difficulty ordering even under slow cooling. More precisely, in a glass the relaxation time scales might diverge exponentially so that the final ($T=0$) size of the correlated regions would grow only like

$$L(T=0) \sim \ln(1/\Gamma), \quad (4.3)$$

where $\Gamma \equiv -dT/dt|_{T=T_{CR}}$ is the cooling rate at $T=T_{CR}$. (For simplicity, we will consider a linear cooling schedule, $T=T_{init}-\Gamma t$, although our results will hold for any cooling schedules, except pathological ones having $\Gamma=0$ or ∞ .)

Does Eq. (4.3) hold for the characteristic length scale in the tiling model? Figure 19 shows the growth of the characteristic length scale L upon cooling at a rate Γ from an initial temperature T_{init} somewhat above T_{CR} . We see that the length scale grows rapidly in a rather small region of temperature below T_{CR} . (Recall that since our method of measuring L is sensitive to thermal fluctuations, the true characteristic length scale is larger than that which is measured at temperatures T close to T_{CR} .) Now let us look at the final length scale reached as a function of Γ , as shown in Fig. 20. Since Fig. 20 is a log-log plot, we expect downward curvature if the depen-

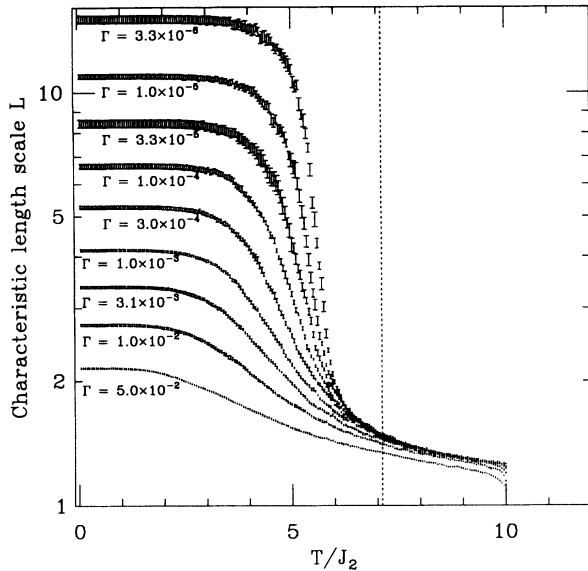


FIG. 19. The growth of the characteristic length scale L for the tiling model during cooling, for various cooling rates Γ . Each set of Monte Carlo data is from an average over 10 runs with error bars giving the standard error. The initial configuration for each run is random ($T = \infty$) and then the system is quenched to either $T = 8J_2$ or $10J_2$, at which point the slower cooling is begun. The transition temperature T_{CR} is marked by the dotted line. (The slowness of the rise in L just below T_{CR} is a consequence of thermal fluctuations causing the characteristic length scale to be underestimated.)

dence of L on $1/\Gamma$ is logarithmic. Clearly this is not the case here. In fact, there is some upward curvature at fast cooling rates with some evidence that the data may be approaching a straight line (power-law dependence) for

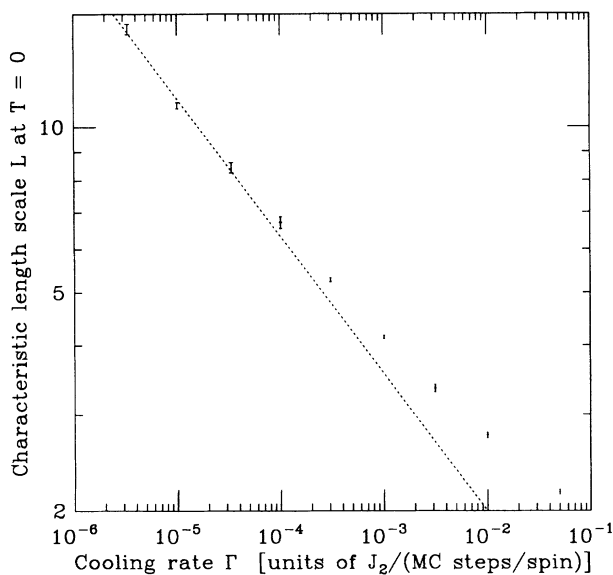


FIG. 20. log-log plot of the length scale L at $T=0$ as a function of the cooling rate Γ . A line of slope $-\frac{1}{4}$ has been drawn suggestively through the data at the lowest cooling rates.

the slowest coolings.

From the point of view of modeling a glassy system, these simulation results are disappointing, though not surprising once we consider the cooling problem more closely. Assuming that, for times t at which $T < T_{CR}$, the characteristic length scale satisfies a differential equation of the form

$$\frac{dL}{dt} \sim \frac{e^{-f_B L/T}}{L^2} \quad (4.4)$$

[with f_B given by Eq. (2.17)], we will now derive an expression for the expected dependence of $L(T=0)$ on the cooling rate Γ which should be valid in the limit of asymptotically slow cooling rate ($\Gamma \rightarrow 0$). This expression will show that (even with the assumption that the barrier to domain growth is proportional to the characteristic length scale) the final length scale on slow cooling should have a power-law, not logarithmic, dependence on the cooling rate, and in this sense the model behaves similarly to models which have been studied by others.⁶⁶ The growing free-energy barriers do, however, change the exponent of the power law from that which we would have expected in their absence.

To start, we note that the characteristic length scale below T_{CR} should initially grow like

$$L(t) \sim t^{1/3}, \quad (4.5)$$

where

$$t = \frac{1}{\Gamma} (T_{CR} - T) \quad (4.6)$$

is the time the system has been below $T = T_{CR}$. However, once the barriers get large, the growth of L will slow dramatically. To a first approximation, we will imagine that there is a sharp cutoff. That is, we assume L grows like Eq. (4.5) down to a certain temperature T_f and then freezes. Figure 19 suggests this approximation is not too bad: The cutoff in the growth of $L(T)$ is quite sharp, particularly at slow cooling rates. Substituting (4.6) with $T = T_f$ into (4.5), we find that

$$L(T_f, \Gamma) \sim \left[\frac{1}{\Gamma} (T_{CR} - T_f) \right]^{1/3}. \quad (4.7)$$

What should we choose for T_f ? One estimate is the temperature at which the ratio of the barrier heights to the temperature is of order 1:

$$\frac{L(T_f, \Gamma) f_B(T_f)}{T_f} = 1. \quad (4.8)$$

This is most certainly an overestimate of T_f , since we expect that L will still be growing when the barriers are this small. A second estimate is to set the time to surmount the barriers equal to the inverse of the cooling rate:

$$e^{L(T_f, \Gamma) f_B(T_f)/T_f} = 1/\Gamma. \quad (4.9)$$

Certainly, we do not expect much further growth once the barriers have gotten this large and, in fact, the growth in L would have already slowed down consider-

ably by this temperature. This is, therefore, probably an underestimate of T_f . We believe these two cutoffs should, in fact, provide rigorous bounds on the asymptotic form of $L(T=0, \Gamma)$.

For now we will use the latter estimate [Eq. (4.9)], although we will find our final result to be very insensitive to the choice of the cutoff T_f . To make further progress, we will also assume

$$\frac{T_{\text{CR}} - T_f}{T_{\text{CR}}} \ll 1. \quad (4.10)$$

This assumption is justified once the cooling rate becomes small, as can be seen from Fig. 19 and will be verified self-consistently at the end of this calculation. We make use of (4.10) to replace T_f by T_{CR} in the denominator of the exponential in Eq. (4.9). We also use (4.10) to write

$$f_B(T_f) = a(T_{\text{CR}} - T_f), \quad (4.11)$$

expressing the fact that the free-energy barrier per unit length grows linearly with decreasing temperature near T_{CR} (see Fig. 7). Substituting (4.11) into (4.9) allows us to solve for $T_{\text{CR}} - T_f$:

$$T_{\text{CR}} - T_f = \frac{T_{\text{CR}}}{aL(T_f, \Gamma)} \ln(1/\Gamma). \quad (4.12)$$

Finally, we substitute (4.12) into our expression for $L(T_f, \Gamma)$, Eq. (4.7), and solve. Making use of our assumption that $L(T=0, \Gamma) = L(T=T_f, \Gamma)$, we arrive at our final result:

$$L(T=0, \Gamma) \sim \left[\frac{\Gamma}{\ln(1/\Gamma)} \right]^{-1/4}. \quad (4.13)$$

If we had used (4.8) instead of (4.9), we would have obtained the same result without the factor of $\ln(1/\Gamma)$. This shows that the result is very insensitive to our exact choice of cutoff and, in particular, that this choice should not change the exponent. Thus, we expect that in the limit $\Gamma \rightarrow 0$, and up to corrections logarithmic in Γ , the characteristic length scale at $T=0$ is⁶⁷

$$L(T=0, \Gamma) \sim \Gamma^{-r} \quad (4.14)$$

with

$$r = \frac{1}{4}. \quad (4.15)$$

Note that if T_f were roughly independent of Γ (as would be true if the barrier heights did not depend upon L), we would have obtained simply $r = \frac{1}{3}$,⁶⁶ since the time t that L has to grow would go like $1/\Gamma$. The change to $r = \frac{1}{4}$ is a nontrivial result of the growing barriers. It reflects the fact that T_f rises toward T_{CR} as the cooling rate becomes smaller, because the larger L means larger barriers at a given temperature.⁶⁸ In fact, Eqs. (4.12) and (4.13) yield

$$T_{\text{CR}} - T_f \sim \Gamma^{1/4}, \quad (4.16)$$

which confirms the validity of assumption (4.10) in the limit $\Gamma \rightarrow 0$.

On the basis of this calculation, we conjecture that, in

general, a free-energy barrier which goes *continuously* to zero at the ordering transition should lead to power-law, and not logarithmic, dependence of the zero-temperature length scale on the cooling rate. This leads us to the conclusion that we need one of two things in order to get a model with length-scale-dependent barriers which behaves like our conception of a glass upon cooling: (i) a free-energy barrier per unit length which jumps discontinuously to a nonzero value at the ordering transition, rather than rising continuously from zero; or (ii) a free-energy barrier per unit length which is nonzero even above the ordering transition. The latter is what is believed to occur in the random-field Ising model.^{1,2} Whether nonrandom models with one or the other of these characteristics exist remains an open question.

V. SUMMARY, CONCLUSIONS, AND OPEN QUESTIONS

The main goal of this paper has been to address the following question: Can we have free-energy barriers to ordering which increase with the size of the correlated regions in a system which does not contain disorder (i.e., randomness in the Hamiltonian)? We have focused our attention on the growth of order in systems far out of equilibrium, in particular, systems which have been quenched from $T = \infty$ (a random state) to a temperature, $T < T_C$, at which the equilibrium phase has long-range order.

Expanding on the work of Lai, Mazenko, and Valls,³ who made the underappreciated point that free-energy barriers proportional to the characteristic length scale will lead to logarithmically slow coarsening, we have given two closely related examples of models, free of randomness in their Hamiltonians, in which such growing free-energy barriers and logarithmic coarsening do, indeed, occur. Although we have not yet been able to rigorously *prove* that the domain growth in the two models is logarithmic, our Monte Carlo results strongly support our heuristic arguments that this is so.

The growing barriers arise because the mechanism by which these systems coarsen involves the creation of a step across a flat interface. Below the corner-rounding transition temperature, T_{CR} , the creation of such a step costs a free energy proportional to its length. Thus, the coarsening dynamics in our 3D model is logarithmically slow only below T_{CR} . In the corresponding equilibrium system, T_{CR} marks an interfacial phase transition involving the rounding of corners on the equilibrium crystal shape. It has long been understood that a connection exists between the roughening transition and the dynamics of crystal growth. The connection between coarsening dynamics and the corner-rounding transition provides a natural extension of the relation between interfacial phase transitions and growth dynamics.

Along the way, we have also studied the 2D Ising model with AFM NNN bonds. This is a particularly clean realization of a system with length-scale-independent activation barriers, and thus serves as a canonical example of such a ‘‘class-2’’ system.³ Finally, we have also discovered (or actually rediscovered⁴⁸) that even the

nearest-neighbor Ising model (no NNN bonds) in three dimensions shows anomalously slow coarsening at zero temperature. This could be just a very long initial transient, but there exists the possibility that the exponent for the growth law is truly smaller (or that scaling breaks down altogether) at $T=0$. This is our one simulation result which still lacks a theoretical understanding.

A. Frustration and the slow growth of order

We believe frustration to be an important feature in producing the slow dynamics. Here we would like to elaborate in what sense we mean “frustration.” The Ising model with NNN bonds is clearly frustrated in the commonly used sense that not all the interactions can simultaneously be satisfied. On the other hand, this frustration does not manifest itself in complicated equilibrium behavior: for $J_1/J_2 > 2d$ (where d is the dimensionality), the ground state is simply ferromagnetic.

In what way then is frustration an important component of our models? The sense of frustration which we are looking for is more of a dynamic one: For the models to lower their free energy they must evolve through states of higher free energy. That is, in order to increase their order on long length scales, the models must first decrease their order on shorter length scales. In the models we have studied here, this “dynamic frustration” comes about because these models prefer sharp domain edges (i.e., no steps), and in order to coarsen, the system must necessarily pass through states in which the domain edges are not sharp. However, it seems likely that one can come up with other ways (still without introducing imposed disorder) to dynamically frustrate a system.

B. Applications to experimental systems

There are two questions which arise in considering the applications of these ideas to experimental systems. Looking most narrowly, we can ask whether there exist systems in which the interactions might lead to slow coarsening of domains. Taking a broader view, we can ponder what our work says more generally about when a system might have diverging barriers associated with a diverging length scale. Since the latter question is what originally got us started on this work, we will consider it first.

1. Relation to the glass transition

The original motivation for this work was to demonstrate the plausibility of our speculations on the glass transition (discussed in Appendix A and, in more detail, in Ref. 69), by searching for models without randomness which nevertheless have free-energy barriers that diverge with the length scale over which the system is ordered. We believe we have found such models. Furthermore, we have also demonstrated the more specific point that a low-temperature ordered phase itself can have slow dynamics. This result is important to explain why the dynamics of a liquid cooled below the glass transition might remain slow even away from the postulated second-order phase transition at T_0 , where the *equilibrium* correlation

length should decrease back down to microscopic values. One might naively expect that this small correlation length means that the ordering dynamics should speed up again, but we have demonstrated a situation in which the relevant length scale with which the barriers diverge is not the equilibrium correlation length, but rather the length scale on which the nonequilibrium system has ordered. Thus, if a system finds itself far out of equilibrium in the low-temperature phase, its dynamics can remain slow even at temperatures well below the transition.

However, in one very important respect the models which we have studied here do not themselves behave as our conception of glasses: they do not have a logarithmic dependence of the final ordering length on the cooling rate. That is, the ordering is not as slow as we would expect when the system is cooled slowly through the ordering transition. The reason, as discussed in Sec. IV D, is that the free-energy barrier per unit length for the tiling model goes continuously to zero as the ordering temperature is approached from below (and for the 3D model, the barrier goes to zero at T_{CR} , a temperature well below the ordering transition). It seems likely from the analysis presented there that any system for which this is true will not show a logarithmic dependence of the length scale on cooling rate.

What do we need in a model to get a real glass? The free-energy barriers in the models of this paper arise purely from *step* free energies. As such, they are expected to go to zero at the transition temperature, as in the tiling model, or even at a lower temperature, as in the 3D model. Our conception of glasses is somewhat different. We imagine that the growing order in a supercooled liquid might consist, for example, of small icosahedrally ordered regions (“balls”). The center of these balls would be most tightly ordered. Further out from the center of each ball, the atoms would be more loosely held because of the frustration induced by trying to fill ordinary space with icosahedral order. Note that, unlike in the models considered in this paper, here the energy density in the ordered regions is not uniform. This nonuniformity is vitally important, since it means that domain walls would like to sit preferentially in gaps between the tightly ordered regions. We believe that moving a domain wall through a tightly ordered region could then cost a free energy proportional to the size of the ordered region even above the ordering transition.

This picture is closely analogous to the random-field Ising model, in which the free-energy barriers are believed to diverge with the diverging correlation length even above T_C .^{2,28} In this model, the nonuniformity is the result of spatial fluctuations in the (quenched) random-field variable. Such fluctuations allow the free-energy barriers per unit size to flipping a domain to retain a nonzero value even above the transition temperature. That similar behavior can occur in a system without disorder remains to be shown.

2. Relation to coarsening in experimental systems

Having discussed the broader question of free-energy barriers which diverge with any ordering length scale, let

us now consider the specific case we have studied, namely, barriers which diverge with the characteristic length scale in a coarsening system. First, we may ask the general question: Has unexplained slow coarsening been seen before in *any* experimental systems? It is usually found that for grain growth in annealed metals and ceramics, the grain size L can be fit reasonably well to the form $L(t) \sim t^n$.⁷⁰ However, the exponent n has often been found to be somewhat (and occasionally, considerably) less than $\frac{1}{2}$, particularly at lower temperatures. On the other hand, it must be remembered that experimental systems can have slow coarsening at low temperatures (and early enough times) simply because, unlike in the Ising model, there are always length-scale-independent barriers involved with the elementary dynamical process of moving atoms around. Furthermore, there has been no general trend for the exponent to decrease at late times (at least, no such trend which cannot be explained trivially by effects such as the finite size of the sample). Also, the general trend has been for the exponent to be lowest in dirty materials and closest to $\frac{1}{2}$ for those of high purity. This suggests that at least many of the observed low exponents are due to impurities.

At this point we should ask whether we have any *specific* reason to expect such grain growth to be logarithmic. In fact, we do not, since grain growth in metals and ceramics differs in several ways from coarsening in the models which we have studied. First, we have no reason to suspect that the interactions in these materials are similar to those in our models. Secondly, in the grain growth problem there is no superimposed lattice structure like we have in our models. Instead, the local orientation of the lattice is determined by the local value of the order parameter within the grain itself.

Rather than just diving headlong into the experimental literature in search of slow growth, let us, instead, look for systems in which the interactions are similar to those of the models we have studied, that is, in which interactions produce domains with sharp edges and corners. Equilibrium crystal shapes have been measured for only a few materials. (For a summary of the experimental difficulties faced in the study of equilibrium crystal shapes, see, e.g., Ref. 39.) Most of the materials studied do not exhibit nonzero edge- and corner-rounding transitions. The edges between facets are rounded at any nonzero temperature (as they are in an Ising model in which the NNN bonds are ferromagnetic or zero). The one exception is the ionic salt sodium chloride, NaCl, whose crystal shape is strictly cubical at low temperatures. In fact, the work of Shi and Wortis³⁸ on the interface model of Sec. IV was motivated by experimental observations⁷¹ of a corner-rounding transition at $T \approx 650^\circ\text{C}$ for NaCl crystals believed to be in equilibrium with their vapor. Furthermore, some earlier experiments on the NaCl crystals actually looked at the coarsening of the [111] interface of a NaCl crystal for temperatures in the vicinity of 650°C .⁷² Pictures of the coarsening interface look strikingly similar to those we obtain for the tiling model.⁷³

Is the slow coarsening dynamics we predict actually seen in these experiments on NaCl? The answer is un-

clear. The coarsening length scale observed after annealing does peak near the corner-rounding transition and then drop at lower temperatures. These experimental observations prompted Shi and Wortis to note that “the fact that coarsening goes away as T is further lowered beyond [the corner-rounding transition temperature] is probably a kinetic effect (slow equilibration at lower temperatures).” This sounds very promising but several strong caveats are in order. The first is again the reminder that in this experimental system there are (coarsening-length-scale-independent) barriers to the elementary process of mass transport which might be large enough to cause slow dynamics over the time scales of the experiment.³⁹ The second caveat is that the time and temperature dependences of the coarsening which are actually reported in the experiments are difficult to interpret. The final caveat is that the range and quality of the experimental results are limited: The experiments were only carried out in a rather narrow range of temperatures within about 25% of the corner-rounding transition. Furthermore, there exists the possibility that surface contamination or other factors played an important role in what was seen. (The experimentalists who studied the equilibrium crystal shape itself⁷¹ note that the degree of coarsening seen in these earlier experiments⁷² is so large as to be inconsistent with their results.)

In the final analysis, we must conclude that while the experiments provide some tantalizing hints that interesting dynamics may be present, we cannot say that they provide either support or refutation for our claim of logarithmically slow coarsening. It seems unlikely that the detailed study of the dynamics necessary to detect the predicted logarithmically slow coarsening will be made unless the experimentalists know what they are looking for. We hope that future experiments on NaCl, or other crystals which have a corner-rounding transition, might look more closely at the dynamics of coarsening of a [111] interface, and particularly at the time dependence of the coarsening length for temperatures not too near the corner-rounding transition. Such experiments will likely prove difficult to perform and it may be hard to separate the effects discussed in this paper from those due to the large elementary energy barriers associated with mass transport. However, we think the rewards of such an experiment make it worthy of the attempt.

C. Open questions

Finally, we would like to leave the reader with some open questions to ponder along two different lines.

(1) How widespread are systems with logarithmically slow coarsening dynamics or, more generally, with free-energy barriers to ordering which diverge with the ordering length scale? Have we found a few systems which are exceptions or are such systems quite common? What features are important in producing such barriers? In what experimental systems might we expect to see slow dynamics?

(2) Can we find models (without randomness) in which the free-energy barriers occur in such a way that they lead to slow ordering dynamics even when a system is

cooled slowly? That is, can we find models which truly fit our conception of glasses?

ACKNOWLEDGMENTS

We are grateful to Veit Elser for suggesting that we study the tiling model discussed in Sec. IV. We also thank David Huse, Peter Nightingale, Teresa Castán, Jennifer Hodgdon, Jacques Amar, and David DiVincenzo for helpful discussions. Finally, J.P.S. would like to thank Daniel Fisher for explaining his scaling ideas about the glass transition, which motivated the work presented here. This work was supported in part by NSF Grant Nos. DMR 88-15685 and DMR 91-18065. Computing facilities were provided in part by the Cornell-IBM Joint Study on Computing for Scientific Research and the Cornell Materials Science Center.

APPENDIX A: SLOW DYNAMICS IN GLASSES

In this appendix, we will briefly discuss our speculations about the glass transition and how these speculations motivated us to search for models which coarsen only logarithmically in time.²⁸

When a liquid is supercooled below its freezing point, it gradually becomes more and more viscous. This continues until some temperature T_g at which the time scales for relaxation become so slow that the liquid can no longer equilibrate on the time scales of the experiment.⁷⁴ For all intents and purposes, the system behaves as a solid, and yet it has no long-range order. It has been aptly described as “a liquid suspended in time.”⁷⁵ We call such a state a glass, and T_g the glass transition temperature.

There has been little discernable progress in understanding the existence of the glass transition despite over half a century of work on the problem. Many theories have been presented but no real consensus seems to be forming. There is one point on which everyone agrees—the “transition” at T_g itself is purely a dynamical phenomenon. In fact, the location of the transition varies with how one chooses to define it. A patient experimentalist who is willing to wait longer to allow the system to relax (i.e., who makes a measurement on a longer time scale) would report a slightly lower value for T_g . For the purposes of uniformity, the location of T_g is conventionally defined as that temperature where the viscosity reaches 10^{13} poise.

But *why* does the liquid become so sluggish? One reason systems become sluggish at low temperatures is because movement of the atoms involves activation over free-energy barriers. In order to test for such activated behavior, one can plot the logarithm of the viscosity η (or any other measure of the relaxation time scale, such as the inverse of the characteristic frequency of dielectric relaxation or of the frequency-dependent specific heat⁷⁶) vs $1/T$.⁶⁹ On such an Arrhenius plot, activation over a constant barrier should produce a straight line. Indeed, for some materials, like SiO_2 , the data can be fit well with a straight line. However, for most other systems there is clear upward curvature on the plot. In fact, it has long been known that viscosity data for glasses can often be fit

reasonably well⁷⁷ with the empirical Vogel-Fulcher (VF) law:

$$\eta = \eta_0 e^{A/(T-T_0)}, \quad (\text{A1})$$

where T_0 is typically tens of degrees below T_g . (For SiO_2 , of course, $T_0=0$ works quite well.)

What physics underlies this empirical law? If we still want to interpret the data within the framework of free-energy barriers to relaxation (which is not the only possible interpretation), we are forced to conclude that the barriers themselves must be increasing as we lower the temperature. If we believe Eq. (A1) holds all the way down to T_0 then the barriers are, in fact, diverging. The Arrhenius law yields Eq. (A1) if the barriers vary with temperature as

$$E_{\text{VF}}(T) = A \left| \frac{T-T_0}{T} \right|^{-\theta}, \quad (\text{A2})$$

where $\theta=1$ gives the VF law exactly, although other powers in the neighborhood of 1 seem to fit data about equally well.

The power-law divergence at T_0 in Eq. (A2) should immediately remind us of the divergences which would occur in many measured quantities if T_0 marked a second-order phase transition, and yet the free-energy barriers to relaxation is not usually one of those quantities which diverges at the transition. In fact, in ordinary second-order phase transitions, it is the time scales to relaxation which diverge with a power law (so-called “critical slowing down”); whereas Eq. (A1) implies that approaching T_0 , time scales are diverging exponentially fast.

Why might barriers be diverging at this transition? Since the correlation length is one of the traditionally divergent quantities at a transition, it seems natural to assume that the barriers may be growing with the size of the correlated regions. In other words, perhaps the supercooled liquid is trying to organize itself into some ordered state, but gets stuck very quickly because of the growth of the barriers.

If such a scenario occurs in nature, why has it not been seen before? The answer to this question is twofold: First, the very existence of such diverging barriers makes a close approach to the equilibrium transition at T_0 impossible since the time scales diverge exponentially fast. The system will necessarily fall out of equilibrium well before reaching T_0 (no matter how patient the experimentalist is). Thus, it is not surprising that these transitions would be among the last to be understood. Secondly, there is, in fact, at least one system in which this scenario *is* believed to occur, namely, the 3D random-field Ising model and its experimental realization, diluted antiferromagnets. The dynamics in these systems is so slow that one can never find the ordered state by cooling and it took a rigorous mathematical proof⁷⁸ to convince skeptics that there is an equilibrium ordered phase at low temperatures.⁷⁹ It has been suggested,^{1,2} and is now generally agreed,³ that the reason the dynamics is so slow is that there are energy barriers to equilibration which diverge with the size of the ordered regions. Similar, but

even more complex, mechanisms may be at work in spin glasses.^{3,80}

However, there is a problem with blissfully applying these ideas to glasses: An important component in all the above-mentioned systems is imposed disorder (i.e., randomness in the Hamiltonian), whereas in glasses, imposed disorder (due to impurities, defects, or the like) is not thought to play a vital role. But is imposed disorder really a necessary condition to get such diverging barriers, or will a weaker condition suffice?

The motivation for the work presented in this paper was to investigate the possibility that frustration without disorder can, at least in some circumstances, produce diverging free-energy barriers to relaxation and the resulting slow dynamics.²¹ We present heuristic arguments and strong numerical evidence for a class of models that have barriers which diverge with the relevant length scale associated with the size of the ordered regions. However, this length scale is not the equilibrium correlation length, but rather the characteristic length scale in a coarsening system, that is, in a system which has been quenched well below its transition temperature. When cooled slowly, our models are not glassy (see Sec. IV D).⁸¹ Nonetheless, the discovery of such slow dynamics for nonrandom coarsening systems is exciting in itself, and is also a large step toward our more ambitious goal of producing models which behave in a glassy manner even when cooled slowly. Finally, it is worth noting that the work presented here, while motivated by our speculative ideas about the glass transition, is in no way dependent upon the correctness of these speculations.

APPENDIX B: CALCULATING THE ENERGY OF CONFIGURATIONS

In this appendix, we briefly describe how we calculate the energy of interface configurations for the 3D Ising model with both J_1 and J_2 bonds. Recall that our convention is that $J_1 > 0$ and $J_2 > 0$ when the NN bonds are ferromagnetic and the NNN bonds are antiferromagnetic. We compute the energy relative to a system with no interface.

Consider a unit area of (microscopic) interface between domains, a “plaquette,” as shown by the shaded square in Fig. 21. Each such plaquette is associated with a broken J_1 bond (energy cost of $2J_1$) which passes through its center. Every plaquette also has two J_2 bonds passing through each of its four edges. Since each of these edges is shared with another plaquette, we associate only four of these eight J_2 bonds with each plaquette. If the plaquette is part of a flat interface then these four antiferromagnetic bonds (which are broken in the bulk) will now be satisfied. We therefore associate with each plaquette an energy cost of $E_p = 2J_1 - 8J_2$.

Note, however, that there is an additional energy associated with each (unit length of) bend in the interface (see Fig. 21). The reason is that along the edge of the plaquette where the bend occurs, only one rather than both the J_2 bonds passing through that edge will be satisfied. This means the energy per unit length of the bend is

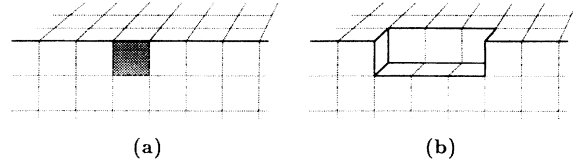


FIG. 21. Two examples of interfaces between domains. We can compute the energies of these interfaces by associating an energy of $E_p = 2J_1 - 8J_2$ with each plaquette of interface (shaded) and an energy of $E_b = 2J_2$ with each unit length of bend (bold solid lines) in the interface. For example, the interface in (b) has 2 more plaquettes and 14 more bends than the interface in (a). Therefore, the energy of (b) is $4J_1 + 12J_2$ higher than the energy of (a).

$$E_b = 2J_2.$$

We now summarize the two rules of energy accounting: (1) each plaquette (unit area of interface) costs an energy $E_p = 2J_1 - 8J_2$, and (2) a bend in the interface costs an energy per unit length of $E_b = 2J_2$. These two rules provide us with a simple understanding of the $T=0$ phase diagram of this model: For $J_1/J_2 < 4$, the ferromagnetic ground state becomes unstable because the energy per plaquette is now negative. This means that it becomes energetically favorable to form interfaces between regions of up and down spins. However, it is still unfavorable to have bends in the interface, which is why the ground state is striped, with alternating planes of up and down spins (and thus flat, planar interfaces).

Also, we can see why the J_2 bonds lead to nonzero edge and corner-rounding transition temperatures. The bend energy $E_b = 2J_2$ produces an attraction between steps, which stabilizes sharp edges and corners up to nonzero temperatures.

APPENDIX C: IMPLEMENTATION OF THE MONTE CARLO ALGORITHM

The standard method of implementing Monte Carlo (MC) dynamics with random updating proceeds as follows: One first chooses a spin at random, and then flips this spin with an “acceptance probability” given by Eq. (1.6). The traditional time unit is one MC step/spin, defined as N such attempts, where N is the number of spins.

This method works very well for temperatures T which are not too small compared to the energy costs ΔE to flip most of the spins, so that the “acceptance rate” (the fraction of the spin-flip attempts which are accepted) is reasonably large. This is definitely not the case in our system. Rather, we are in the limit where almost all the attempted flips will be rejected because most of the spins have large energy costs $\Delta E \gg T$ to flipping. For such situations, a much more efficient algorithm has been proposed by Bortz, Kalos, and Lebowitz,⁸² the so-called “continuous time” Monte Carlo method. It has been used previously to study coarsening in Potts models.¹³ The basic insight leading to continuous time MC is that

the standard MC method is hampered by its fixed time step. When few energetically favorable flips are possible, the standard MC must adjust by lowering its acceptance rate, whereas what one would like to do is to keep the rate of acceptance high and, instead, compensate by incrementing the time step by a larger amount. By doing this correctly, one can actually make every attempt a successful flip. The method proceeds as follows.

(1) Add together the acceptance probabilities for all the spins in order to obtain a total flip rate Γ . Increment the time by an amount τ (in MC steps/spin) where τ is a random number chosen from an exponential distribution with mean $1/\Gamma$.

(2) Choose a spin, with the probability for a given spin to be chosen equal to its fractional contribution to the total rate. Thus, spin i with acceptance probability Γ_i will be chosen with probability Γ_i/Γ .

(3) Flip this spin and go back to step 1.

The drawback of this method is that each such flip entails quite a bit of overhead, particularly in step (2). In actual practice, as Bortz *et al.* pointed out, the algorithm can be speeded up by sorting the spins into classes. The idea is that at the start of a run one classifies each spin according to the number of nearest neighbors and next-nearest neighbors aligned with it. (For the 3D model, there are 91 such classes.) One then keeps a table of the acceptance probability for a spin in each class. The total rate Γ_j for a class j is then this acceptance probability multiplied by the number of spins in the class. Choosing which spin to flip is now done in two stages. First, a class j is chosen with probability Γ_j/Γ . Then which spin in this class to flip is chosen totally at random (since all have an equal acceptance probability). One then reclassifies this spin and its nearest and next-nearest neighbors, calculates the resulting change in the total rate Γ , and repeats the procedure of incrementing the time and choosing the next spin to flip.

When the acceptance probabilities are high, this method still has enough additional overhead to make it slower than the standard method. Therefore, for coarsening simulations we have often employed a hybrid of the two algorithms: At short times when the domains are small and the acceptance rate for the standard MC method is high, we use the standard method. At later times, we switch over to the continuous time method. At the latest times, the savings over the standard method can be *very* substantial. For example, in a system of

40 000 spins, there may be an average of less than one successful flip per time unit (i.e., the acceptance rate for the standard method is less than 1 in 10^4).

The two methods yield equivalent results. This can be seen by noting that for both methods, the ratio of the occurrence of flipping two spins is given by the ratio of their acceptance probabilities. Also, for both methods, the total number of flips per time step will, on average, be given by Γ , the sum of all the acceptance probabilities. At early times, we have compared the two methods numerically and find that they do indeed give equivalent results within statistical errors.

APPENDIX D: SCALING AND ANISOTROPY OF THE CORRELATION FUNCTION

Here, we present a short discussion of Monte Carlo results for the scaling properties of the correlation function, $C(\mathbf{r}, t)$, for the model discussed in Secs. I–III. The scaling hypothesis states that at late times the correlation function $C(\mathbf{r}, t)$ is not a function of \mathbf{r} and t separately, but rather depends only on the ratio $\mathbf{r}/L(t)$:

$$C(\mathbf{r}, t) = \tilde{C}[\mathbf{r}/L(t)]. \quad (\text{D1})$$

The term “scaling” is also used to refer to the stronger statement one makes by replacing $L(t)$ with its asymptotic form t^n , i.e.,

$$C(\mathbf{r}, t) = \tilde{C}(\mathbf{r}/t^n). \quad (\text{D2})$$

In the case of our 3D model, we would replace t^n in Eq. (D2) by $\ln(t)$. However, we know such a form will not hold very well for our data since we are just beginning to see the expected asymptotic behavior of $L(t)$ at the latest times reached. Thus, we shall concentrate on determining whether we can see the weaker form of scaling implied by Eq. (D1).

We are also interested in the existence of anisotropy in the correlation function. To investigate this, we look at the correlation function along a few different directions. In two dimensions, we consider it along the lattice axes and along the lattice diagonals. In three dimensions, we look along the lattice directions, the face diagonals ([110] direction), and the body diagonals ([111] direction). As an example, here is the explicit definition we use for the correlation function along the face diagonals in three dimensions:

$$C_{[110]}(\sqrt{2}r) = \frac{1}{6N} \sum_i \{ s(\mathbf{r}_i) s[\mathbf{r}_i + (\hat{\mathbf{x}} + \hat{\mathbf{y}})r] + s(\mathbf{r}_i) s[\mathbf{r}_i + (\hat{\mathbf{x}} - \hat{\mathbf{y}})r] + s(\mathbf{r}_i) s[\mathbf{r}_i + (\hat{\mathbf{y}} + \hat{\mathbf{z}})r] + s(\mathbf{r}_i) s[\mathbf{r}_i + (\hat{\mathbf{y}} - \hat{\mathbf{z}})r] \\ + s(\mathbf{r}_i) s[\mathbf{r}_i + (\hat{\mathbf{z}} + \hat{\mathbf{x}})r] + s(\mathbf{r}_i) s[\mathbf{r}_i + (\hat{\mathbf{z}} - \hat{\mathbf{x}})r] \}, \quad (\text{D3})$$

where $s(\mathbf{r}_i)$ is the value of the Ising spin at the location \mathbf{r}_i , and r is a non-negative integer. (The trivial dependence on time has been suppressed for brevity.)

It is important to notice that our measure of $L(t)$, Eq. (3.1), is inversely proportional to $C_{[100]}(0) - C_{[100]}(1)$ (using the notation for the 3D case). Thus, when we mea-

sure $L(t)$ in this way, we are studying the initial slope of the correlation function in the direction of the lattice axes. This has important implications for the scaling plots to be presented below: When we plot $C_{[100]}(r, t)$ vs $r/L(t)$, we are forcing the initial slopes of the correlation function at different times to be equal. Therefore, we will

necessarily see good scaling near the origin. This limits the extent to which we can determine whether or not scaling is satisfied, particularly when we look at $C(r,t)$ along the lattice axes.

For the 2D nearest-neighbor ($J_2=0$) Ising model, Humayun and Bray⁸³ have recently tested scaling with extensive simulations on systems of size 1000^2 . They find that scaling is well obeyed and furthermore that there is no evidence for anisotropy in the scaling function [i.e., scaling plots for $C(r,t)$ along the lattice axes and along the lattice diagonals fall on top of one another]. As a check on our numerics, we have repeated this calculation on 500^2 systems and find the same results.²⁹

Let us now consider scaling in the 2D model for $J_2 \neq 0$. Figure 22 shows results for two values of T/J_2 . There are three points to be made. First, there is little or no difference seen for the two values of T/J_2 . Second, unlike the case of $J_2=0$, here we can clearly see anisotropy in the correlation function. This should not surprise us given the “blocky” appearance of the configurations. However, we believe that this anisotropy should disappear once $L(t) \gg e^{4J_2/T}$, in which case the domain boundaries should have a significant number of kinks in them. For the two temperatures which we have shown in Fig. 22, we are always in the regime $L(t) < e^{4J_2/T}$. We have

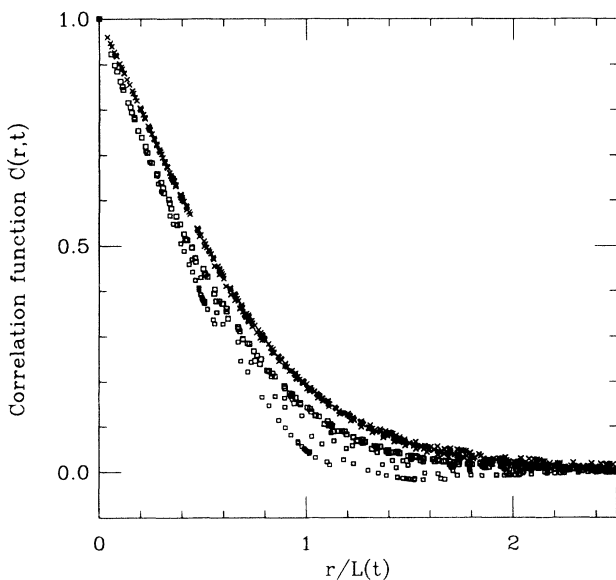


FIG. 22. Scaling and anisotropy in two dimensions. This shows a scaling collapse of the correlation function, $C(r,t)$, for the 2D Ising model. The collapse is achieved by plotting $C(r,t)$ vs $r/L(t)$. Results are given for $T=0.42J_2$ and $0.72J_2$ from 30 runs each on a 400^2 system. The correlation function along both the lattice axes (\times) and the diagonals (\square) is plotted. [$C(r,t)$ is shown at 18 times ($10 \leq t \leq 2 \times 10^6$ MC steps/spin) and 12 times ($10 \leq t \leq 2 \times 10^4$ MC steps/spin) for $T=0.42J_2$ and $0.72J_2$, respectively. The late-time data along the diagonals ($t \geq 2 \times 10^5$ MC steps/spin for $T=0.42J_2$, and $t \geq 2400$ MC steps/spin for $T=0.72J_2$) are shown by larger squares than earlier time data.] There is clearly anisotropy in the correlation function at these temperatures out to the latest times studied. See text for a discussion of scaling.

investigated the anisotropy at two higher temperatures, $T=1.8J_2$ and $T=3.6J_2$.²⁹ Particularly for the latter, we can get out to the regime $L(t) \gg e^{4J_2/T}$, and we find the anisotropy is indeed less pronounced, particularly at later times. However, the shift in the curves with time is quite small and there is still some detectable anisotropy even at the latest times [where $L(t) \approx 30$] for both temperatures.

The third point concerns scaling: When we look only along the lattice axes, the correlation function appears to scale fairly well over all times. However, we have explained above why this is a rather poor test of scaling. When we look instead along the lattice diagonals, scaling is fairly good only at late times, once the $t^{1/2}$ growth of $L(t)$ has resumed (although, as noted above, we would predict that the curves should continue to shift very slowly to the right over time to reduce the anisotropy). At earlier times the correlation function does not satisfy scaling, with the curves lying clearly to the left of those at later times.

Finally, we look at scaling in the 3D model for $J_2 \neq 0$. Figure 23 shows a scaling plot for the correlation function for $T=2J_2$ and $T=3J_2$ along the lattice axes; and for only $T=3J_2$ along the face and body diagonals. As in two dimensions, we can clearly see anisotropy in the correlation function. We conjecture that, unlike what we expect in two dimensions, here this anisotropy will remain out to all times. Along the lattice axes, the collapse of the data appears to be quite good (besides a little

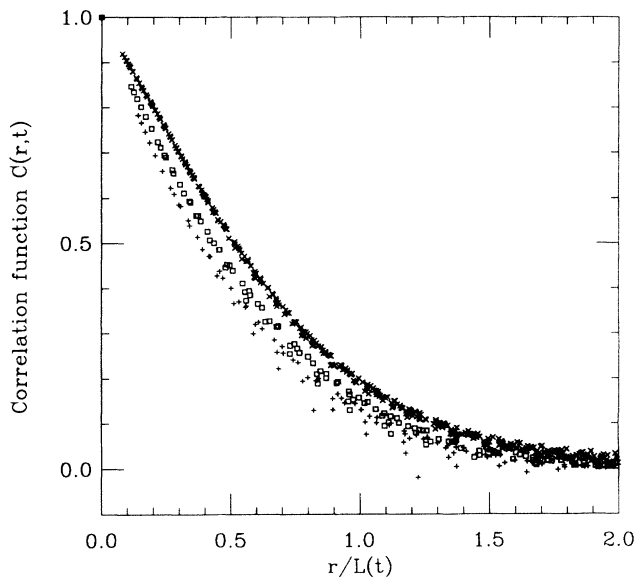


FIG. 23. Scaling and anisotropy in three dimensions. This shows a scaling collapse of the correlation function, $C(r,t)$, for the 3D model along the lattice axes (\times), face diagonals (\square), and body diagonals ($+$), for $T=2J_2$ in an 80^3 system, averaged over 20 runs. The collapse is achieved by plotting $C(r,t)$ vs $r/L(t)$. Results at 14 times ($10 \leq t \leq 80000$ MC steps/spin) are included. Also included for the case of the lattice axes are results for $T=2J_2$, in an 80^3 system averaged over 10 runs, at 18 times ($10 \leq t \leq 2 \times 10^6$ MC steps/spin). Anisotropy in the correlation function is clearly apparent. See text for a discussion of scaling.

deviation upward in the tails at the latest few times, probably as a result of finite-size effects), and there is no perceivable dependence on the value of T/J_2 . However, in the diagonal directions, there is a tendency for the data at early times (say, $t \leq 650$ MC steps/spin) to lie below and to the left of the later time data, gradually approaching it as time increases. For the later times, scaling is quite good. This suggests that the scaling regime for $T = 3J_2$ is not reached until $t \approx 10^3$ MC steps/spin. This is about the same time when the growth in $L(t)$ begins to look roughly logarithmic.

The conclusion from our studies of the correlation functions is that, at late times, scaling [in the weaker

sense of Eq. (D1)] appears to be satisfied in two and three dimensions even when $J_2 \neq 0$. However, our results are certainly not sensitive enough to preclude the possibility of small deviations from scaling. At earlier times, there are some deviations from scaling. These are likely due to the fact that the NNN AFM bonds, in slowing the growth of $L(t)$, also slow the approach to the scaling regime. The one clear result of the NNN bonds is to make the correlation function anisotropic. This is not surprising given the blockiness of the configurations when $J_2 \neq 0$. Our conjecture is that this anisotropy will remain in the 3D model out to all times, while in the 2D model the anisotropy will slowly decrease once $L(t) \gg e^{4J_2/T}$.

*Present address: Department of Physics, Simon Fraser University, Burnaby, British Columbia, Canada V5A 1S6.

¹G. Grinstein and J. F. Fernandez, Phys. Rev. B **29**, 6389 (1984).

²D. S. Fisher, Phys. Rev. Lett. **56**, 416 (1986).

³Z. W. Lai, G. F. Mazenko, and O. T. Valls, Phys. Rev. B **37**, 9481 (1988).

⁴J. D. Shore and J. P. Sethna, Phys. Rev. B **43**, 3782 (1991).

⁵J. D. Shore, J. P. Sethna, M. Holzer, and V. Elser, in *Slow Dynamics in Condensed Matter*, AIP Conf. Proc. No. 256, edited by K. Kawasaki, M. Tokuyama, and T. Kawakatsu (AIP, New York, 1992), p. 541.

⁶For a more detailed discussion, see Ref. 29. For a detailed early review of the field, see J. D. Gunton, M. San Miguel, and P. S. Sahni, in *Phase Transitions and Critical Phenomena*, edited by C. Domb and J. L. Lebowitz (Academic, New York, 1983), Vol. 8, p. 269. For a recent collection of theoretical and experimental articles on coarsening see *Dynamics of Ordering Processes in Condensed Matter*, edited by S. Komura and H. Furukawa (Plenum, New York, 1988).

⁷I. M. Lifshitz, Zh. Eksp. Teor. Fiz. **42**, 1354 (1962) [Sov. Phys. JETP **15**, 939 (1962)].

⁸S. M. Allen and J. W. Cahn, Acta. Metall. **27**, 1085 (1979).

⁹I. M. Lifshitz and V. V. Slyozov, J. Phys. Chem. Solids **19**, 35 (1961); E. M. Lifshitz and L. P. Pitaevskii, *Physical Kinetics*, Landau and Lifshitz: Course of Theoretical Physics Vol. 10 (Pergamon, Oxford, 1981).

¹⁰S. A. Safran, Phys. Rev. Lett. **46**, 1581 (1981).

¹¹G. F. Mazenko, O. T. Valls, and F. C. Zhang, Phys. Rev. B **31**, 4453 (1985); **32**, 5807 (1985); G. F. Mazenko and O. T. Valls, *ibid.* **33**, 1823 (1986).

¹²In the case of the Potts model, whether or not such freezing occurs depends on the lattice and on the range of the interactions (Refs. 13 and 14).

¹³G. S. Grest, M. P. Anderson, and D. J. Srolovitz, Phys. Rev. B **38**, 4752 (1988).

¹⁴J. Viñals and M. Grant, Phys. Rev. B **36**, 7036 (1987).

¹⁵D. A. Huse, Phys. Rev. B **34**, 7845 (1986).

¹⁶J. G. Amar, F. E. Sullivan, and R. D. Mountain, Phys. Rev. B **37**, 196 (1988).

¹⁷C. Roland and M. Grant, Phys. Rev. B **39**, 11971 (1989).

¹⁸For example, in Ref. 13, Grest *et al.* consider further-neighbor interactions in the 3D Potts model with the justification that they want to avoid zero-temperature freezing due to local lattice effects in order to better study the universal features of the domain growth. Our claim is that it is possible for such lattice effects to alter the universal features, that is, to change the asymptotic growth law for the model. Do we expect the nearest-neighbor 3D Potts model to

have logarithmic coarsening? There are special configurations which have an energy cost per unit length involved in expanding any of the domains along that boundary. On the other hand, it is not at all clear that such configurations will form with sufficient probability to pin the coarsening system. Therefore, we are not sure what to expect, but believe it is *possible* that the model does not coarsen as $t^{1/2}$.

¹⁹See, e.g., J. Viñals and D. Jasnow, Phys. Rev. B **37**, 9582 (1988); C. Jeppesen, H. Flyvbjerg, and O. G. Mouritsen, *ibid.* **40**, 9070 (1989). Recently, however, Mouritsen and co-workers have made a claim of logarithmic coarsening in a model without randomness, namely a 2D Ising model with diffusing (i.e., annealed) vacancies [P. J. Shah and O. G. Mouritsen, Phys. Rev. B **41**, 7003 (1990)]. Their claim is based upon numerical simulations of such a coarsening system. Gregory Hassold and David Srolovitz have disputed this claim [G. N. Hassold and D. J. Srolovitz (private communication)] since they have seen similar slowing of the growth for diffusing impurities in their grain growth (Potts model) simulations, but with a return to $t^{1/2}$ behavior at later times.

²⁰These classes should not be confused with the universality classes which distinguish the different scaling behaviors at long times. For example, classes 1 and 2 here both correspond to the same universality class.

²¹We consider our models to be frustrated in a dynamical sense: In order for the system to lower its energy in the long run, it must go through states of higher energy in the short run (see Sec. V A).

²²For equilibrium properties of the 2D model, see J. Oitmaa, J. Phys. A **14**, 1159 (1981); D. P. Landau and K. Binder, Phys. Rev. B **31**, 5946 (1985), and references therein.

²³We generalize this to zero temperature by taking the limit $T \rightarrow 0$ in Eq. (1.6), which gives $P=0$, $\frac{1}{2}$, or 1, if $\Delta E > 0$, $\Delta E = 0$, or $\Delta E < 0$, respectively.

²⁴R. J. Glauber, J. Math. Phys. **4**, 294 (1963).

²⁵N. Metropolis, A. W. Rosenbluth, M. N. Rosenbluth, A. H. Teller, and E. Teller, J. Chem. Phys. **21**, 1087 (1954).

²⁶The 2D model also serves the pedagogical purpose of being a particularly clean example of a class-2 system, since there is only a single barrier height ($4J_2$).

²⁷C. Rottman and M. Wortis, Phys. Rev. B **29**, 328 (1984); Phys. Rep. **103**, 59 (1984).

²⁸For a more detailed discussion of the slow dynamics in glasses and our theoretical views on the matter, see Ref. 69. That paper (and the abbreviated discussion here) presents an elaboration of scaling ideas about the glass transition suggested to us

- by Daniel Fisher [D. S. Fisher (private communication)].
- ²⁹J. D. Shore, Ph.D. thesis, Cornell University, 1992.
- ³⁰In the simulation, the first edge is considered to have flipped when the J_1 energy first falls below its initial value. We choose to show this time rather than the time to shrink the cubic domain entirely because it is easier to compare with analytic calculations. The time to shrink the entire domain behaves similarly (see Ref. 4, Fig. 1). At any rate, the time to flip an edge is certainly a lower bound on the time to shrink the entire cube and is, in fact, quite a good bound in the low-temperature limit where the time to shrink the cube is dominated by the time to flip the first edge.
- ³¹The factor of 2 accounts for the fact that, for each edge, spins can be flipped on either of the two adjoining faces. The -1 corrects for the double counting of the lowest barrier configuration [Fig. 4(a)].
- ³²A cruder estimate of $T_{CR} \approx 9-10J_2$ reported in Ref. 4 was obtained from calculating f_B to only second order in $e^{-4J_2/T}$.
- ³³W. K. Burton, N. Cabrera, and F. C. Frank, *Philos. Trans. R. Soc. London, Ser. A* **243**, 299 (1951).
- ³⁴J. D. Weeks, G. H. Gilmer, and H. J. Leamy, *Phys. Rev. Lett.* **31**, 549 (1973).
- ³⁵H. van Beijeren and I. Nolden, in *Structure and Dynamics of Surfaces II*, edited by W. Schommers and P. vonBlanckenhagen, Topics in Current Physics Vol. 43 (Springer-Verlag, Berlin, 1987), p. 259.
- ³⁶M. Holzer and M. Wortis, *Phys. Rev. B* **40**, 11 044 (1989).
- ³⁷In practice, we compute step free energies without explicitly specifying the step orientation. This means that we sum over all possible orientations and thus get the step free energy for the step with the most probable orientation (M. Holzer, Ph.D. thesis, Simon Fraser University, 1990).
- ³⁸A.-C. Shi and M. Wortis, *Phys. Rev. B* **37**, 7793 (1988).
- ³⁹M. Wortis, in *Chemistry and Physics of Solid Surfaces VII*, edited by R. Vanselow and H. F. Howe (Springer-Verlag, Berlin, 1988), p. 367.
- ⁴⁰In Refs. 27, 38, and 39, the authors use T_0 and T_3 to denote the corner- and edge-rounding transition temperatures, respectively. Note that the tricritical temperature T_t discussed in Ref. 27 is no longer believed to exist (as explained in Ref. 39).
- ⁴¹In Ref. 4, we did not fully appreciate the connection of our work with the work on equilibrium crystal shapes and, as a result, referred to both these transition temperatures as “edge-roughening” temperatures. We called T_{ER} the roughening temperature for an infinite edge, and identified T_{CR} as the roughening temperature for a finite edge (i.e., an edge which ends in a corner).
- ⁴²In detail, the barrier free energy is related to the step free energy as follows: Unlike the step free energy, the barrier free energy is calculated not per unit length of step, but per unit length of step *as projected* onto one of the lattice axes (i.e., per unit length of cube edge). We perform this calculation by summing over all configurations without any restrictions on the average orientation of the step. In the thermodynamic limit, we therefore calculate the barrier free energy per unit projected length for the most probable orientation of such a step/barrier. The most probable orientation with respect to the crystal axes, θ , is easily computed to be
- $$\tan[\theta(T)] = \frac{x^2}{(1-x)(1-x+x^2)},$$
- where $x \equiv \exp(-4J_2/T)$. Our barrier free energy is nothing but the step free energy for a step of orientation θ , modulo a geometric factor of $\cos(\theta)$ which accounts for the projection.
- ⁴³It is perhaps worth emphasizing that our justification for the claim does not come from imagining that the cubes we shrink are themselves equilibrium crystal shapes. In fact, they should not be thought of as equilibrium objects at all.
- ⁴⁴For example, for the Potts model on a triangular lattice, one can identify metastable configurations, that is, configurations in which there are energy barriers to any possible state change. However, in the coarsening process, these metastable configurations are not nucleated in sufficient number to pin the entire system and the model coarsens (i.e., it does not freeze) at $T=0$. [S. A. Safran, P. S. Sahni, and G. S. Grest, *Phys. Rev. B* **28**, 2693 (1983); P. S. Sahni, D. J. Srolovitz, G. S. Grest, M. P. Anderson, and S. A. Safran, *ibid.* **28**, 2705 (1983); Viñals and Grant (Ref. 14).]
- ⁴⁵D. Stauffer, *Introduction to Percolation Theory* (Taylor and Francis, London, 1985).
- ⁴⁶D. Chowdhury, M. Grant, and J. D. Gunton, *Phys. Rev. B* **35**, 6792 (1987).
- ⁴⁷Reference 46 notes the importance of using the equilibrium energy E_{eq} , rather than the ground-state energy E_0 , in Eq. (3.1), in order to correct for thermal fluctuations. However, here we will be working in the limit of $T \ll T_C$, so, to an excellent approximation, $E_{eq} = E_0$.
- ⁴⁸J. G. Amar and F. Family, *Bull. Am. Phys. Soc.* **34**, 491 (1989); (private communication).
- ⁴⁹M. P. Anderson, D. J. Srolovitz, G. S. Grest, and P. S. Sahni, *Acta Metall.* **32**, 783 (1984).
- ⁵⁰G. S. Grest and D. J. Srolovitz, *Phys. Rev. B* **32**, 3014 (1985).
- ⁵¹Such a form does introduce a third parameter, L_0 , obtained as a constant of integration. However, we perform the fits keeping the parameter L_0 fixed. The fits are good as long as L_0 is fixed at some reasonable value (e.g., $L_0=1$ or 3 work equally well). Furthermore, we find that fits to the form derived from integrating the equation analogous to Eq. (3.2), but without the $1/L$ factor (and again with L_0 fixed to 1 or 3), give fits almost indistinguishable from those to the form $L(t) = a \ln(t/t_0)$. This suggests that it is not the introduction of a third parameter, but rather the more accurate portrayal of the physics, which leads to the superior fits obtained from Eq. (3.2).
- ⁵²It is worth emphasizing that the observation of blocky configurations does not in itself imply logarithmic growth. It is this blockiness together with the argument that such blocky configurations will have barriers which grow with the length scale that supports our logarithmic growth hypothesis. [Whereas, in 2D, the blocky configurations that we observe do not have barriers which grow with length scale, and, in fact, we expect the blockiness in 2D to decrease once $L(t)$ gets very large (see Appendix D).]
- ⁵³See, e.g., Ref. 14. They discuss a 2D system, where one can have strips infinite in one dimension. In a 3D system, one can have both tubes (infinite in one dimension) and slabs (infinite in two dimensions).
- ⁵⁴Alternatively, one might be tempted to argue that we should change our definition of $L(t)$ [Eq. (3.1)] by defining $E_0^{NN} \equiv (-3N + 6\mathcal{L}^2)J_1$, which is the lowest value of the nearest-neighbor energy that the system can have with antiperiodic boundary conditions. However, this is *not* correct since we want to define $L(t)$ as being inversely proportional to the total domain perimeter, regardless of boundary conditions. For any remaining skeptics, we note that if we do use $E_0^{NN} \equiv (-3N + 6\mathcal{L}^2)J_1$ in Eq. (3.1), we find that the simulation results for $L(t)$ have a strong dependence on the system size even at early times, whereas, using $E_0^{NN} \equiv -3NJ_1$ gives

- results independent of system size (until times late enough that finite-size effects are obviously important).
- ⁵⁵H. W. J. Blöte and H. J. Hilhorst, *J. Phys. A* **15**, L631 (1982); B. Nienhuis, H. J. Hilhorst, and H. W. J. Blöte, *ibid.* **17**, 3559 (1984). These authors considered a model with the same tiling configurations but with a different Hamiltonian.
- ⁵⁶V. Elser (private communication).
- ⁵⁷The average orientation of the interface is controlled by the relative number of each type of tile. We will only be interested in the case of equal numbers of each tile, i.e., in a [111] interface.
- ⁵⁸The boundary between unlike tiles corresponds to a bend in the interface, which costs an energy of $2J_2$ per unit length (see Appendix B).
- ⁵⁹C. Jayaprakash and W. F. Saam, *Phys. Rev. B* **30**, 3916 (1984).
- ⁶⁰The point is that, from the three-dimensional viewpoint, digging a hole in, or building upon, a flat ([100], [010], or [001]) section of interface will necessarily produce some hidden interface, when viewed from the [111] direction.
- ⁶¹Reconstructions of this type have an extensive literature. [C. Herring, *Phys. Rev.* **82**, 87 (1951); in *Structure and Properties of Solid Surfaces*, edited by R. Gomer and C. S. Smith (University of Chicago Press, Chicago, 1953), p. 5. For reviews, see A. J. W. Moore, in *Metal Surfaces: Structure, Energetics, and Kinetics* (American Society for Metals, Metals Park, OH, 1963), p. 155; M. Flytzani-Stephanopoulos and L. D. Schmidt, *Prog. Surf. Sci.* **9**, 83 (1979).] They are referred to by several different names, including “hill-valley reconstruction,” “Herring reconstruction,” “thermal etching,” and “thermal faceting.”
- ⁶²For the tiling model, the activation barriers can be studied by looking at the time to shrink a “cubical projection.” Such a Monte Carlo study has been conducted (Ref. 29) and yields results qualitatively similar to those shown in Fig. 3.
- ⁶³By infinite temperature, we mean that $T/J_2 \rightarrow \infty$, keeping $T/J_1 = 0$, i.e., the initial state must be a tiling. Such an initial tiling cannot be produced by simply choosing a random spin configuration, since such a configuration will not, in general, correspond to a tiling at all. We prepare the $T = \infty$ initial state as follows: First, we tile the plane with the elementary hexagons (i.e., the shaded objects in Fig. 14), with each hexagon chosen randomly to be in one of the two possible orientations. Such a tiling is not a $T = \infty$ state, however, since its entropy is clearly not maximized. We randomize this tiling by randomly flipping spins which have three of their six nearest neighbors aligned (during which time the average energy of the system decreases). We perform this randomization for at least 100 MC steps/spins, by which time the average energy has leveled off.
- ⁶⁴Note that we do *not* define $E_0 \equiv (-N + 8\sqrt{N})J_2$, which is the lowest energy state that can be reached by this system (given the boundary conditions and the restriction that the number of each type of tile remain equal). See Ref. 54.
- ⁶⁵For example, in previous work on coarsening (Ref. 46), it has been suggested that an approximate way to correct for the effects of thermal fluctuations is to use the equilibrium energy E_{eq} , rather than the ground-state energy E_0 , in the definition of $L(t)$ [Eq. (4.2)]. However, below T_{CR} , the tiling model is thermodynamically frozen with $E_{\text{eq}} = E_0$. Out of equilibrium, the thermal fluctuations are dependent on $L(t)$ itself, so that there seems to be no such obvious way to correct our measure of $L(t)$.
- ⁶⁶S. J. Cornell, K. Kaski, and R. B. Stinchcombe [*Phys. Rev. B* **45**, 2725 (1992)] have studied ordering under slow cooling in a 2D Ising model with Glauber dynamics and barriers that *do not* diverge with length scale; they argue that $L \sim \Gamma^{-1/2}$, as we would expect. However, the general prediction they make [their Eq. (29)] fails for our model because of the diverging barriers. Studies of slow cooling have also been carried out in several 1D models. [R. Schilling, *J. Stat. Phys.* **53**, 1227 (1988); W. Kob and R. Schilling, *J. Phys. A* **23**, 4673 (1990); J. Jackle, R. B. Stinchcombe, and S. Cornell, *J. Stat. Phys.* **62**, 425 (1991); S. J. Cornell, K. Kaski, and R. B. Stinchcombe, *J. Phys. A* **24**, L865 (1991); *Phys. Rev. B* **44**, 12263 (1991).] Since these models have their phase transitions at zero temperature, critical slowing down and the nontrivial behavior of the equilibrium correlation length can lead to a variety of different exponents (see also Ref. 81).
- ⁶⁷Numerical integration of (4.4) (with a linear cooling schedule) also yields $L(T=0, \Gamma) \sim \Gamma^{-1/4}$ as $\Gamma \rightarrow 0$. This confirms the validity of the approximations we made in deriving (4.14) and (4.15) from (4.4).
- ⁶⁸What determines r is the value of the exponent n which would *naively* describe the coarsening system (i.e., $n = \frac{1}{3}$ for conserved order parameter, or $\frac{1}{2}$ for nonconserved order parameter) and the value of the exponent m describing the behavior of f_B as the ordering transition is approached from below: $f_B(T) \sim (T_{\text{CR}} - T)^m$. If one generalizes our argument to general m and n , one finds $r = mn/(n+m)$. However, it is unclear to us whether this would hold in the case of a second-order transition, where there are fluctuations on all length scales in the equilibrium system as one approaches the transition.
- ⁶⁹J. P. Sethna, J. D. Shore, and M. Huang, *Phys. Rev. B* **44**, 4943 (1991).
- ⁷⁰Summaries of the experimental literature on grain growth can be found in Ref. 49; M. P. Anderson, G. S. Grest, and D. J. Srolovitz, *Philos. Mag.* **B 59**, 293 (1989), Table 2; V. Randle, B. Ralph, and N. Hansen, in *Annealing Processes—Recovery, Recrystallization, and Grain Growth*, edited by N. Hansen, D. Juul Jensen, T. Leffers, and B. Ralph (Risø National Laboratory, Risø, 1986), p. 123; H. Hu and B. B. Bath, *Metal. Trans.* **1**, 3181 (1970).
- ⁷¹J. C. Heyraud and J. J. Métois, *J. Cryst. Growth* **84**, 503 (1987).
- ⁷²D. Knoppik and A. Losch, *J. Cryst. Growth* **34**, 332 (1976); D. Knoppik and F.-P. Penningsfeld, *ibid.* **37**, 69 (1977).
- ⁷³There is a large body of related experimental work on other systems in which an unstable interface coarsens by some sort of hill-valley reconstruction into pieces of interface of allowed orientations (see Ref. 61). Unfortunately, the field remains somewhat murky, with many of the experimental results in contradiction with one another. In particular, it is not clear how close to equilibrium the surfaces are in many of the experiments.
- ⁷⁴We use the concept of equilibrium in a rough sense here, since clearly a supercooled liquid is never in true equilibrium. What interests us, however, is not the ordered solid state that would have been formed (which we will assume is thermodynamically inaccessible), but rather the metastable liquid state. We say that the liquid falls out of equilibrium when it can no longer “equilibrate” in the sense of following the free-energy minimum of this metastable state.
- ⁷⁵S. Brawer, *Relaxation in Viscous Liquids and Glasses* (The American Ceramic Society, Columbus, OH, 1985).
- ⁷⁶P. K. Dixon and S. R. Nagel, *Phys. Rev. Lett.* **61**, 341 (1988); P. K. Dixon, *Phys. Rev. B* **42**, 8179 (1990).
- ⁷⁷It is not always possible to fit to the VF law over the entire

range of viscosity with one set of values for the parameters. The controversy over the extent to which the viscosity and other data really do obey the VF law, along with alternate fits to the data and theories of the glass transition, are discussed further in Ref. 69. See also Ref. 76.

⁷⁸J. Z. Imbrie, *Phys. Rev. Lett.* **53**, 1747 (1984); *Commun. Math. Phys.* **98**, 145 (1985).

⁷⁹A very readable account of the controversy, written at a time just before it was finally settled, is given by G. Grinstein, *J. Appl. Phys.* **55**, 2371 (1984).

⁸⁰D. S. Fisher and D. A. Huse, *Phys. Rev. Lett.* **56**, 1601 (1986).

⁸¹For related work on a model which does show glassy behavior upon slow cooling (and, in fact, a correlation length which

grows only as the logarithm of the logarithm of the cooling rate), see S. L. Shumway and J. P. Sethna, *Phys. Rev. Lett.* **67**, 995 (1991); S. L. Shumway, Ph.D. thesis, Cornell University, 1991. That model, however, has its phase transition at zero temperature, whereas to model a glass we are looking for such slow growth of order associated with a nonzero transition temperature, T_0 .

⁸²A. B. Bortz, M. H. Kalos, and J. L. Lebowitz, *J. Comput. Phys.* **17**, 10 (1975). See also, K. Binder, in *Monte Carlo Methods in Statistical Physics*, edited by K. Binder, 2nd ed. (Springer-Verlag, Berlin, 1986), Sec. 1.3.1.

⁸³K. Humayun and A. J. Bray, *J. Phys. A* **24**, 1915 (1991).

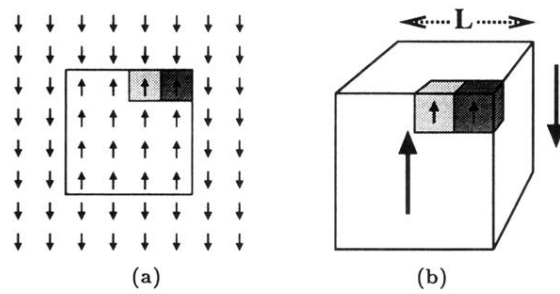


FIG. 1. (a) A square domain of “up” spins in a system of “down” spins, in two dimensions. The next-nearest-neighbor bonds introduce an energy barrier of $4J_2$ to flipping a corner spin (dark gray). As a result, it takes a time of order $e^{4J_2/T}$ to shrink the entire domain. (b) A cubic domain in three dimensions. (Here, for clarity, most of the individual spins have not been shown.) There is an energy barrier of $12J_2$ to flip a corner spin (dark gray) and a barrier of $4J_2$ to flip each spin along the edge (light gray). Thus, unlike in two dimensions, the total barrier to flip all the spins along an edge is proportional to the linear size, L , of the domain; and the time to shrink the domain is now exponential in L .

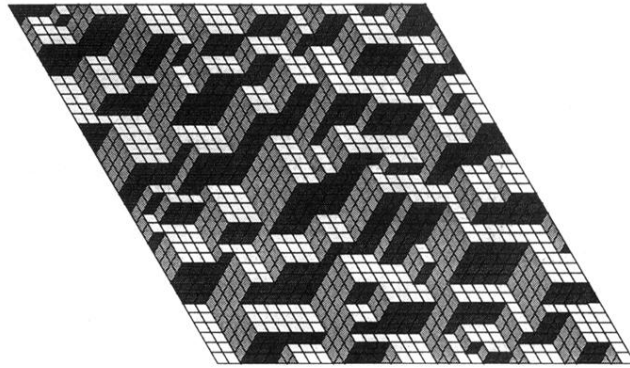


FIG. 12. A sample configuration for the tiling model. Viewed from the $[111]$ direction, an interface in a 3D model can be represented by a tiling of the plane by rhombi of three orientations, provided that the interface has no overhangs when thus viewed. (We have shaded the three types of rhombi differently in order to distinguish them more easily and enhance the 3D perspective.) If we assign an energy of $2J_2$ to each unit length of boundary between the different types of tiles, then the energetics of this model matches that of the 3D Ising model with next-nearest-neighbor antiferromagnetic bonds.

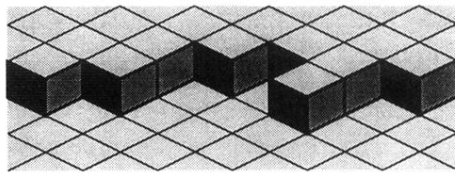


FIG. 13. An example of an interface configuration which cannot be represented by the tiling model. Part of the interface is hidden from view (i.e., there is an “overhang”) and this results in some incomplete (triangular) tiles.

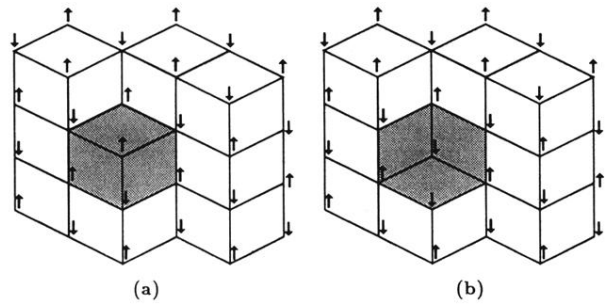


FIG. 14. The elementary dynamical move in the tiling model. In the 2D spin representation, the move consists of flipping a spin which has exactly three of its six nearest neighbors aligned. In tiling language, it consists of a rotation of an elementary hexagon (shaded) by 60° . From a 3D perspective, we see that it represents an elementary cube either added or taken away.

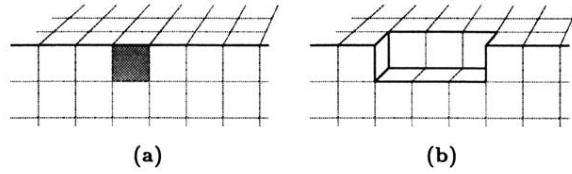


FIG. 21. Two examples of interfaces between domains. We can compute the energies of these interfaces by associating an energy of $E_p = 2J_1 - 8J_2$ with each plaquette of interface (shaded) and an energy of $E_b = 2J_2$ with each unit length of bend (bold solid lines) in the interface. For example, the interface in (b) has 2 more plaquettes and 14 more bends than the interface in (a). Therefore, the energy of (b) is $4J_1 + 12J_2$ higher than the energy of (a).